ISTANBUL TECHNICAL UNIVERSITY ★ GRADUATE SCHOOL OF SCIENCE ENGINEERING AND TECHNOLOGY

INFLUENCE OF HALLOYSITE NANOTUBES ON THE MECHANICAL AND THERMAL PROPERTIES OF EPDM NANOCOMPOSITES

M.Sc. THESIS

Yağmur POLAT

Department of Polymer Science and Technology

Polymer Science and Technology Programme

MAY 2014

ISTANBUL TECHNICAL UNIVERSITY ★ GRADUATE SCHOOL OF SCIENCE ENGINEERING AND TECHNOLOGY

INFLUENCE OF HALLOYSITE NANOTUBES ON THE MECHANICAL AND THERMAL PROPERTIES OF EPDM NANOCOMPOSITES

M.Sc. THESIS

Yağmur POLAT
(515111045)

Department of Polymer Science and Technology

Polymer Science and Technology Programme

Thesis Advisor: Prof. Dr. Nurseli UYANIK

MAY 2014

İSTANBUL TEKNİK ÜNİVERSİTESİ ★ FEN BİLİMLERİ ENSTİTÜSÜ

HALOYSİT NANOTÜPLERİNİN EPDM NANOKOMPOZİTLERİN MEKANİK VE TERMAL ÖZELLİKLERİNE ETKİSİ

YÜKSEK LİSANS TEZİ

Yağmur POLAT
(515111045)

Polimer Bilim ve Teknolojileri

Polimer Bilim ve Teknolojileri Programı

Tez Danışmanı: Prof. Dr. Nurseli UYANIK
Anabilim Dalı : Herhangi Mühendislik, Bilim
Programı : Herhangi Program

MAYIS 2014

Yağmur POLAT, a **M.Sc.** student of ITU **Graduate School of Science Engineering and Technology** student ID **515111045**, successfully defended the **thesis** entitled "**INFLUENCE OF HALLOYSITE NANOTUBES ON THE MECHANICAL AND THERMAL PROPERTIES OF EPDM NANOCOMPOSITES**", which she prepared after fulfilling the requirements specified in the associated legislations, before the jury whose signatures are below.

Thesis Advisor :	**Prof. Dr. Nurseli UYANIK** Istanbul Technical University	.....
Jury Members :	**Prof. Dr. Nurseli UYANIK**	.....
	Prof. Dr. Ayfer SARAÇ	.....
	Assoc. Prof. Dr. Orhan GÜNEY	.....

Date of Submission : 5 May 2014
Date of Defense : 29 May 2014

To my family,

FOREWORD

First of all, I would like to express my gratitude to my thesis advisor Prof. Dr. Nurseli UYANIK, for her academic instructions and all the support during this thesis.

I would like to give my special thanks to Mehmet Ali ÇAKIROĞLU and ARSAN KAUÇUK PLASTİK-MAKİNA SAN. TİC. A.Ş. workers for technical and EPDM rubber supporting of during my thesis studying.

I also would like to show my appreciation to Tuğba UÇAR DEMİR and Adnan ALTAS from ESAN Company for supporting of halloysite nanotubes and providing X-Ray diffraction analysis of my samples.

I also thank Refik ARAT for Thermogravimetry Analysis measurements of my study.

My personal thanks are to Mustafa AKSAKAL for his guidance and to my friends Tanya Hazal KAYSOYDU, Emine ATAGÜN, Asier De CELIS HERNÀNDEZ and Umut Baran ÖZSUYU for their fellowship.

Most importantly, I wish to express a special debt of gratitude to my family, especially my mother Neslihan Elif UÇKAN, my father Çetin POLAT, my brother Hasan Kaan POLAT and Feridun UÇKAN for their encouragement and supporting my decisions through all my life.

May 2014

Yağmur POLAT
(Chemist)

TABLE OF CONTENTS

ABBREVIATIONS

ACN : Acrylonitrile
BIIR : Bromobutyl Rubber
BR : Polybutadiene
CB : Carbon Black
CLD : Crosslinking Density
CIIR : Chlorobutyl Rubber
CNFs : Carbon Nanofibers
CNTs : Carbon Nanotubes
CR : Polychloroprene
CRI : Cure Rate Index
C2 : Ethylene Content
DCPD : Dicyclopentadiene
EACM : Ethylene-Acrylic Rubber
ENB : Ethylidene Norbornene
EPDM : Ethylene Propylene Diene Monomer
EPDM-g-MA : Maleic Anhydride Modified Ethylene-Propylene Diene Monomer
EPM : Ethylene Propylene Monomer
HNTs : Halloysite Nanotubes
IIR : Butyl Rubber
IISRP : Institute of Synthetic Rubber Producers
IR : Synthetic Polyisoprene Ethylene Content
IRHD : International Rubber Hardness Degrees Tester
K6950 : Keltan 6950
K778Z : Keltan 778Z
NR : Natural Rubber
MDR : Moving Die Rheometer
MV : Mooney viscometer
M_H : Maximum Viscosity
M_L : Minimum Viscosity
M_L (1+4) : Mooney Viscosity
MMT : Montmorillonite Organoclay
MU : Mooney Unit
MW : Molecular Weight
MWD : Molecular Weight Distribution
M100 : Tensile Modulus at 100% Elongation
NBR : Nitrile Rubber
PE : Polyethylene
phr : Per Hundred Rubber
PNCs : Polymer Nanocomposites
PP : Polypropylene
Q : Silicone Rubber

SBR **:** Styrene-Butadiene Rubber
SR **:** Synthetic Rubber
SSBR **:** Solution SBR
TAC **:** Triallyl Cyanurate
TGA **:** Thermal Gravimetric Analyser
TPE **:** Thermoplastic Elastomer
TPO **:** Thermoplastic Olefin
ts_2 **:** Scorch Time
t_{90} **:** Optimum Curing Time
XRD **:** X-ray Diffraction
1,4 - HD **:** 1,4 Hexadien

LIST OF TABLES

Page

LIST OF FIGURES

INFLUENCE OF HALLOYSITE NANOTUBES ON THE MECHANICAL AND THERMAL PROPERTIES OF EPDM NANOCOMPOSITES

SUMMARY

Rubbers, which are typical elastomers, are capable of rapid elastic recovery after being stretched to at least twice its length from -18 °C to 66 °C at any humidity. Ethylene-propylene rubbers (EPM) are the copolymer of ethylene and propylene copolymers that one of the fast improved and more studied synthetic rubbers in last five decades. Because of absence of double bonds in the structure of EPM rubbers, they have a saturated backbone, which explains their excellent weatherability, ozone resistance and oxidation resistance. On the other hand, because of saturated backbone, they cannot be vulcanized with sulfur. EPM rubbers vulcanization can occur with peroxide or radiation. On the purpose of dealing with this situation, a diene structure were reacted as a pendant group to main chain and created a termonomer (ethylene-propylene diene monomer). The three important principal parameters for ethylene-propylene diene monomer (EPDM) are molecular weight (Mooney viscosity), ethylene/propylene ratio and type of termonomer. Mooney viscosity affects processability of EPDM compound. Ethylene/propylene ratio determines crystallinity of EPDM compound which increases by increasing of ethylene content. Increasing of crystallinity provides better mechanical properties, more crosslinking density and higher capacity for filler load in EPDM matrix. Fillers are important components for a rubber compound. They are used to have good processability, reduction of cost and better mechanical properties for rubber compounds. Nanoclays can be also used as filler. Rubber scientists has been studying on a novel filler, halloysite nanotubes (HNTs). HNTs has a similar chemical structure ($Al_2Si_2O_5(OH)_4.nH_2O$) with kaolinite. However, HNTs differs from kaolinite because of its original hollow tubular shape and intermolecular water. HNTs with large aspect ratio that are eco-friendly fillers, improve mechanical and thermal properties of polymers.

In this study, two kinds of EPDM, Keltan 778Z with ethylene content of 67%, ethylidene norbornene (ENB) of 4.3% and Keltan 6950 with ethylene content of 48%, ENB of 9%, were mixed with HNTs that were used as filler to prepare EPDM/HNTs nanocomposites by using laboratory type two-roll mill. Four different compounds were prepared with HNTs and without HNTs for each kind of EPDM. HNTs amounts were between 0-40 phr in each of EPDM matrixes. The test results were investigated due to ethylene/propylene ratios and the amount of HNTs in the nanocomposites. Densities of EPDM/HNTs samples were measured to decide weight of sample that would be put into hot pres. Before vulcanization of EPDM/HNTs compounds, Mooney viscometer (MV) and moving die rheometer (MDR) were used to find Mooney viscosity ($M_L(1+4)$) at 100 °C and to evaluate curing times and curing parameters (maximum viscosity and minimum viscosity) of EPDM/HNTs compounds at 192 °C, respectively. The curing times decreased by increasing of HNTs content of both Keltan778Z/HNTs and Keltan6950/HNTs compounds up to 10

phr, where a maximum cure times were observed. The maximum torque and minimum torque values are corresponded to maximum viscosity (M_H) and minimum viscosity (M_L) of compounds during curing. Due to HNTs contents of EPDM/HNTs compounds and kinds of EPDM, M_H and M_L showed changes. Moreover, M_L (1+4) of EPDM/HNTs compounds increased by increasing of HNTs content. Curing process was practiced by using basic two plates, single cavity compression mold hot press in MDR defined times for each compound at 192 °C. The cured 2 mm thickness of EPDM/HNTs nanocomposites samples were used for mechanical, thermal and morphological tests. Mechanical properties of EPDM/HNTs nanocomposites (tensile strength, elongation at break, tensile modulus) were investigated by using universal tensile testing machine. The test results showed that HNTs content and ethylene-propylene ratio of EPDMs had a marked effect on the tensile properties of HNT filled EPDM rubbers. Crosslinking density (CLD) values of EPDM/HNTs nanocomposites were calculated with an equation by using tensile modulus value. Compression set apparatus was used to practice deformation processes. In addition, nanocomposite samples were subjected to rubber aging test for certain time at 70 °C. After aging test, nanocomposite samples were put to tensile tests to compare pre-aging and post-aging states. Hardness of initial and post-aging states of nanocomposites were measured by using Shore A type durometer and international rubber hardness degrees tester (IRHD). Thermal gravimetric analyser (TGA) was used to have an opinion about thermal stability and composition of nanocomposite samples. According to TGA test results after decomposition of nanocomposite samples, weight of residue increased by increasing HNT content in nanocomposites. The temperatures at which EPDM/HNTs nanocomposites started to decompose, varied due to HNTs content and sort of EPDM. Morphological properties were observed by using X-ray diffraction (XRD) analyser that provided observing of the basal spacings of HNTs.

HALOYSİT NANOTÜPLERİNİN EPDM NANOKOMPOZİTLERİN MEKANİK VE TERMAL ÖZELLİKLERİNE ETKİSİ

ÖZET

Endüstride kullanılan polimerler üç alt sınıfta toplanmaktadırlar: Plastikler, elastomerler ve elyaflar. Kauçuk, moleküllerinin dizilişi ve göstermiş olduğu mekanik davranış açısından elastomer sınıfının üyesidir. Kauçuk ilk olarak Amerika yerlileri tarafından günlük hayatlarında su geçirmeyen giysi, ve çocukların oynadıkları top yapımında kullanıldı. Kauçuğun süte benzer görünümlü ham maddesi Brezilya kökenli Hevea Brasiliensis ağacından elde ediliyordu. Fransız bilim adamı La Condamine'nin yaptığı başarılı bilimsel çalışmalarla, Avrupalıların kauçuğu tanımaları ve endüstride kullanmaları başlamıştır. Brezilya kökenli kauçuk ağacının tohumları İngiltere'de yetiştirilmeye başlandı; Seylan ve Malezya'da kauçuk çiftlikleri kuruldu. Kauçuk başlangıçta sıcakta yumuşayıp yapışkan hale geliyor; soğukta ise sertleşip kırılgan oluyordu. Bu da bu malzemenin kullanımını kısıtlıyordu. 1839 yılında Charles Goodyear'ın vulkanizasyon işlemini bulmasına kadar termoplastik elastomer olan kauçuk türü malzemeler, vulkanizasyon işleminden sonra kimyasal yapılarında geri dönüşümsüz değişiklik meydana gelen (çapraz bağlanma reaksiyonu), termoset elastomer grubunda yer aldı. Vulkanizasyon prosesi ile yapışkan olmayan, yüksek mukavemetli, düşük kalıcı deformasyonlu, ısıdan az etkilenen, elastik özellikler ve kolay işlenme gibi pozitif özelliklere sahip olan kauçuk, sanayide bir çok alanda kullanılmaya başlanmıştır. Son yıllarda yapılan çalışma ve araştırmalar göstermiştir ki etilen-propilen kauçukları (EPM) en hızlı gelişen ve yaygınlaşan sentetik kauçuklardan biridir. Ticari olarak ilk kez 1961 yılında üretilmeye başlanan EPM kauçukları, etilen ve propilenin kopolimerizasyonu sonucu elde edilmektedir. Kimyasal yapılarında çift bağ bulunmadığından, tamamen doymuş özellikteki EPM kauçuk ozona ve oksijene karşı mükemmel dayanıklılık göstermektedir. Vulkanizasyon işlemleri peroksit ve radyasyon ile gerçekleştirilebilir. Ancak doymuş yapılarından dolayı kükürt ve kükürt verici sistemler ile vulkanizasyon gerçekleştirilemez ve bu sistemlerle vulkanize olan diğer kauçuklarla kıyaslanmaları mümkün olamaz. Daha sonraları etilen ve propilen ile üçüncü monomer olarak bir dien reaksiyona sokulmuş; terpolimer olan etilen-propilen dien monomeri (EPDM) elde edilmiştir. Bu durum diğer kauçuk türleriyle kıyası ve peroksit dışında kükürt ve kükürt verici sistemlerle de vulkanizasyonu olanaklı kılmıştır. EPDM'in ticari olarak ilk üretimi 1963 yılında başlamıştır. Sahip olduğu avantajlar sayesinde geniş bir uygulama alanına sahip olup, genel maksatlı bir kauçuk türü haline gelmiştir. Tabii kauçuğun mekanik özelliklerini (yüksek elastikiyet, genleşme, çekme mukavemeti, sıcağa-soğuğa karşı direnç), ihtiyacın olduğu uygulama alanına göre değiştirmek mümkün değildir. Sentetik kauçukta ise, kimyagerin kauçuğun hammaddelerini ve moleküler yapısını, yani polimer yapı tarzını amaca ve kullanım alanı gereksinimlerine uygun olarak değiştirmesi imkanı vardır. Kullanılacak EPDM'in seçiminde üç temel bileşim faktörü vardır: molekül

ağırlığı (Mooney viskozite), etilen/propilen oranı ve termonomer cinsi ve miktarı. Mooney viskozite, EPDM karışımının işlenebilirliği hakkında bilgi verir. Yüksek Mooney viskozitesine sahip EPDM karışımları kapalı karıştırıcılarda, düşük Mooney viskozitesine sahip karışımlar ise açık karıştırıcılarda karıştırılır. Buna ilaveten EPDM karışımının yüksek Mooney viskozitesine sahip olması, bu karışımın dar molekül ağırlığı dağılımına sahip olduğu anlamına gelmektedir. Ayrıca EPDM kauçuklarının Mooney viskozite değeri arttıkça yağ ve dolgu maddesi alma kapasiteleri de artmaktadır. Ticari olarak üretilen EPDM kauçuğunun molekül ağırlığı 200000-300000, Mooney viskozite değerleri (M_L (1+4)) ise 100 °C'de 25-100 MU değerleri arasında değişmektedir. Etilen-propilen oranı EP(D)M kauçuğun kristalinitesini etkilemektedir. %45-60 arası etilene sahip olan bir EP(D)M kauçuk amorf yapıdadır ve mekanik özellikleri, kauçuk direnci düşüktür. Ancak etilen oranı %70-80 olan EP(D)M kauçukta uzun etilen zincirleri görülür ve bu düzen kristaliniteyi artırır. Kristalinitenin artması ile mekanik özellikler, çapraz bağ yoğunluğu ve dolgu kabul edilebilirlikte de artış gözlenir. EPM kauçuklarının doymuş yapılarından dolayı kükürt ve kükürt verici vulkanizasyon ajanlarıyla vulkanizasyon işlemi yapılamıyordu. Bu durumun üstesinden gelmek için ve aynı zamanda bu kararlı yapıyı da bozmamak adına etilen-propilen monomerlerine ek olarak üçüncü bir dien monomeri yan grup olarak eklenmiştir. EPDM kauçuklarının %4-5'ini oluşturan bu dien yapıları vulkanizasyon hızını önemli ölçüde etkilemektedirler. Ticari olarak kullanılan başlıca üç farklı termonomer vardır: 1,4 hekzadien (1,4 - HD), disiklopentadien (DCPD) ve etiliden norbornen (ENB). Kauçuk karışımları kauçuk maddesinin yanı sıra gereken miktarlarda katkı maddeleri de içermektedirler. Katkı maddeleri, karışımın uygulanacağı prosese elverişli hale getirilmesi ve bitmiş mamulün uygulama alanına uygun özellikler taşıması amacıyla kullanılırlar. Dolgu maddeleri, yumuşatıcılar, proses kolaylaştırıcılar, yaşlanmayı geciktiriciler ve vulkanizasyon sisteminde kullanılan aktivatörler, hızlandırıcılar, pişiriciler, geciktiriciler birer katkı maddesidir. EPDM kauçukların yapılarında bulunan doymamışlık ısı, ışık, ve ozon gibi dış etkenlere karşı polimerin dirençli olmasını sağlar. Böylece herhangi bir antioksidant, antiozonat kullanımı gerekmez. Dolgu maddeleri kauçuk karışımları için önemli bir bileşendir. Temelde güçlendirici olan ve güçlendirici olmayan olmak üzere iki ana gruba ayrılırlar. Bu maddeler kauçuğun işlenebilirliğinin artırılması, maliyetin düşürülmesi, mekanik özelliklerin iyileştirilmesi ve polimer ağırlığının azaltılması amacıyla kullanılırlar. Sentetik kauçuk üretiminde en çok kullanılan dolgu maddesi karbon siyahıdır. EPDM kauçukları yüksek miktarda dolgu maddesini alabilme özelliğine sahiptirler. Diğer kauçuk türlerinde olduğu gibi EPDM kauçuklarında da karbon siyah dolgu maddesi kullanımı oldukça yaygındır. Mineral dolgular (talk, kaolin kili, montmorillonit kili) da renkli malzeme üretiminde ya da karbon siyah maliyetini düşürmek amacıyla karbon siyahına katılarak kullanabilirler. Mineral dolgular, kauçuğa kattıkları özelliklere göre yarı kuvvetlendirici, kuvvetlendirici ve doldurucu olarak görev alabilirler. Son yıllarda çevreye dost kil dolgu maddelerine olan ilgi artmıştır. Bilim insanları özellikle sahip oldukları avantajlardan dolayı nano boyutta partiküllere sahip inorganik yapıdaki killerin dolgu maddesi olarak kullanılmasıyla ilgili pek çok çalışma yapmışlardır; ve de hala çalışmaya devam etmektedirler. Kauçuklara dolgu maddesi olarak eklenen nano boyutlu dolgu maddeleri kauçukların daha iyi mekanik ve termal özelliklere, alev geciktiriciliğe, iyileştirilmiş gaz geçirgenliğine sahip olmalarını sağlar. Nano dolgu maddesi olarak karbon nanotüpler (CNT) yaygın bir şekilde kullanılmaktadır. Ancak 21. yüzyılda daha da önem kazanan yeşil teknoloji akımı ile çevreye dost, insana ve doğaya zararı asgari boyutta olan yeni maddeler

üzerine çalışmalar artmıştır. Haloysit nanotüp (HNT) bunlardan biridir. HNT katkılı kauçuklarla ilgili çalışmalar oldukça ilgi çekicidir. Kimyasal içerik ($Al_2Si_2(OH)_4.nH_2O$) olarak kaolinitle birbirlerine çok benzeseler de yapısal olarak farklıdırlar. Haloysit içi oyuk, tüpsü yapılardan meydana gelmektedir. Tüpsü yapıların iç yüzeyi alüminat, dış yüzeyi silikat yapılarından oluşmaktadır. HNT doğaya ve insan sağlığına dost olmasının yanında, maliyeti yüksek olan katkı maddelerinin kullanım miktarını azaltması, biyouyumlu olması ve kauçuğun mekanik davranışları iyileştirici etkisine sahip olması gibi avantajlara da sahiptir.

Bu çalışmada, dolgu maddesi olarak kullanılan HNT'nin, etilen/propilen oranları birbirinden farklı iki EPDM polimeri (Keltan 778 Z ve Keltan 6950) üzerindeki mekanik, termal ve morfolojik etkileri karşılaştırılmıştır. Keltan 778Z içeriği %67 etilen ve %4,3 ENB iken; Keltan 6950 içeriği %48 etilen ve %9 ENB'dir. Vulkanizasyon işlemi peroksit ortamında gerçekleştirilmiştir. Her bir EPDM çeşidinden bir takım oluşturulmuş; HNT 0-40 phr arasında kullanılmıştır. Her bir takım için 4 farklı HNT phr değeri kullanılmış; toplamda 8 örnekle çalışılmıştır. Reçete içeriği laboratuvar tipi çift merdaneli karıştırıcıda karıştırılmıştır. Belli bir hacimdeki sıcak presin alabileceği örnek miktarını hesaplamak için yoğunluk ölçme işlemi gerçekleştirildi. Vulkanizasyon işleminden henüz geçmemiş olan hamur karışımlarına öncelikle reometre ve Mooney viskozite testleri yapılmıştır. Karışımların pişme zamanları (ts_2, t_{90}) ve pişme ile ilgili parametreleri (M_L ve M_H) reometre test cihazında 192 °C'de tespit edilmiştir. 0 phr HNT ile diğer farklı miktarlarda HNT içeren karışımların reometre test sonuçları kıyaslandığında pişirme hızının 10 phr değerine kadar yavaşladığı; ancak 10 phr değerinden sonra hızlandığı görülmüştür. Karışımların reometre testi sonucu elde edilen maksimum viskozite (M_H) ve minimum viskozite (M_L) değerlerinde değişiklikler gözlenmiştir. Karışımların Mooney viskozite (M_L (1+4)) ölçümleri ise Mooney viskometre ile 100 °C'de gerçekleştirilmiştir. Pişme süreleri, pişme parametreleri ve M_L (1+4) değerleri etilen/propil oranına (iki polimer aynı miktardaki HNT'lere göre kıyaslandığında) ve HNT miktarlarına göre (aynı takımdaki örnekler birbirleri ile kıyaslandığında) değişiklik göstermiştir. Karışımların vulkanizasyonu reometre testinde elde edilen pişirme sürelerine göre sıcak preste gerçekleştirilmiştir. Preste karışımların pişirilmesiyle elde edilen 2 mm kalınlığındaki EPDM/HNT nanokompozit plakaları, vulkanizasyon sonrası yapılacak testlerde kullanılmıştır. Nanokompozit plakalar, mekanik testlerin belli bir standarda göre yapılabilmesi için standart boyutlarda papyon şeklinde kesilerek hazırlanmıştır. Nanokompozit örneklerinin mekanik özellikleri (kopma mukavemeti, kopma uzaması, elastisite modülü) 500 mm/min test hızında çekme testiyle incelenmiştir. Nanokompozit örneklerinin çapraz bağ yoğunlukları elastisite modülünün kullanıldığı bir eşitlikle bulunmuştur. 6 mm kalınlığında hazırlanan nanokompozit örneklerinin 70 °C sıcaklıkta 24 saat boyunca kompresyon set ölçümleri alınmış; kalıcı deformasyon yüzdeleri tayin edilmiştir. Buna ilaveten, nanokompozit örnekleri 70 °C'de 168 saat boyunca tutularak, yaşlanma testine tabi tutulmuşlardır. Nanokompozit örneklerinin sertlikleri yaşlandırma öncesi ve sonrası Shore A tipi durometre ve IRHD tipi sertlik ölçüm cihazı ile ölçülerek kıyaslanmıştır. HNT miktarlarına ve etilen/propilen oranlarına göre elde edilen sertlik değerleri farklılık göstermiştir. Nanokompozit örnekleri yaşlandırma sonrasında da çekme testine tabi tutulmuş; kopma mukavemeti ve kopma uzaması değerleri kıyaslanmıştır. Termogravimetrik analiz yöntemi ile nanokompozit örneklerinin termal kararlılıkları ve karışım kompozisyonu hakkında fikir edinilmiştir. Test bitiminde bozunmaya uğrayan nanokompozitlerden geriye kalan kül miktarının HNT miktarıyla orantılı bir şekilde arttığı gözlemlenmiştir.

Nanokompozitlerin bozunmaya başladıkları sıcaklıklar HNT oranına ve EPDM çeşidine göre farklılık göstermiştir. Nanokompozit örneklerin morfolojik özellikleri X-ışını kırınım (XRD) cihazı ile incelenmiştir. XRD ile HNT'lerin tüpsü yapısından kaynaklanan tabakalar arası açıklıklar hesaplanmıştır.

1. INTRODUCTION

Ethylene propylene diene monomer (EPDM) is a type of synthetic terpolymer rubber [1]. The ethylene content (C2) is generally between 40% and 80%. The diene content is generally between 0% and 10% [2]. Increasing of C2 ratio value contributes to crystallinity of EPDM. Higher level of the diene monomer (ethylidene norbornene-ENB) brings about faster cure rate [3]. EPDM rubbers are good at electrical insulation and they have good resistance to heat, UV, ozone, and oxidation.

The main reason for adding fillers into rubbers is to enhance the chemical and physical properties, and latter is saving the amount of polymer, as well as to reduce cost and weight of the compounds. Fillers in polymers are used as a reinforcement agent, which impart enhancement on thermal and mechanical properties and reduce their costs and weights [4]. Nanoclays are also used as reinforcement agents [5]. However high cost and difficulty of their process controls make researchers concentrate on different nanoclays reinforcements, such as halloysite nanotubes (HNTs). Halloysite is two layered aluminosilicate with hollow nanotubular structure [6]. HNTs with large aspect ratio improve mechanical and thermal properties of polymers. Halloysite is defined chemically as ($Al_2Si_2O_5(OH)_4.nH_2O$) just as kaolinite [7]. On the other hand halloysite is distinguished from kaolinite, because of its original tubular shape.

In this work, two kinds of EPDMs (Keltan 778Z and Keltan 6950), which had different C2 and ENB ratios, were used for the nanocomposite samples productions. HNTs were used as nano-filler to improve mechanical and thermal properties of EPDM rubber. HNTs with from 0 to 40 phr values were added to the EPDM rubber samples and mixed on laboratory type two-roll mill. For peroxy curing, Perkadox 14.40B was used. The test results were evaluated depending on the C2 ratios of EPDM and the contents of HNT in the nanocomposites. The effects of HNT loading on Keltan 778Z (ethylene content of 67%, ENB of 4.3%) and Keltan 6950 (ethylene content of 48%, ENB of 9%) nanocomposites were characterized mechanically and thermally. Curing properties (M_L and M_H) and curing times (scorch time - ts_2,

optimum curing time - t_{90}) of uncured samples at 192 ^{0}C were examined by moving die rheometer (MDR). Mooney viscosity (M_L (1+4)) was measured by the Mooney viscometer (MV). Densities of compounds were measured to calculate weight of them which were put to mould and cure in hot press. Curing and molding (compression) processes of compounds were carried out by hot press during optimum cure time at 192 °C. Mechanical properties of nanocomposites samples (i.e. tensile strength, elongation at break, tensile modulus) were examined by using universal testing machine. Crosslinking densities (CLD) of nanocomposites were calculated by use of tensile modulus at 100% elongation (M100) values. Deformation processes were practiced by use of compression set apparatus. Shore durometer and international rubber hardness degrees tester (IRHD) were used to measure hardness of initial and post-aging states of nanocomposites. Thermal gravimetric analysis (TGA) was used to determine the thermal properties of nanocomposite samples. X-Ray diffraction analyses of HNT and EPDM/HNT nanocomposites were performed to see the basal spacing of the HNTs before and after blending with EPDM.

2. THEORETICAL PART

2.1 Historical Review of Rubber

Natural rubber (NR) obtained from trees was the only source of rubber until the invention of the synthetic polymers in the early part of the twentieth century. When explorer Christopher Columbus arrived in Haiti in 1492, he found American Indians playing a game with a rough bouncing ball made from latex of certain trees; and the latex oozed out of those trees when their bark was cut. American Indians were also known to have used latex for making footwear, bottles, and cloaks. By 1735, latex had been described as *caoutchouc* by a French geographical expedition in South America [8]. The elasticity and waterproofing ability of the material inspired interest of the scientists in Europe. The English scientist Joseph Priestley coined the word 'Rubber', because the material could rub out pencil marks. In the early days, rubber products behavior was like thermoplastics, which became hard in winter, and soft and sticky in summer. So in this case, the interest in rubber was limited, for example, to water proof textiles, because the material became soft, tacky under heat, and brittle at lower temperatures [9]. Charles Goodyear worked with NR for a long time. Initially, he tried to improve its properties, using different kind of metal salts. After meeting Nathanial Hayward and learning about his experiments on mixing NR and sulfur, Goodyear was assigned Hayward's patent US 1090. In the winter of 1838/39, Charles Goodyear discovered that when rubber was heated with sulphur, it became stronger and more elastic, but above all, it was not sensitive to changes in temperature. This process was became known as vulcanization (from 'Vulcan', the God of Fire). In 1844, he patented the vulcanization process in several countries [10].

In 1888, the pneumatic tire was patented by John Dunlop in England. In 1910, B.F. Goodrich Company invented longer life tires by adding carbon to the rubber [9]. In 1911, Philip Strauss invented the first successful tire, which was a combination tire and air filled inner tube. Because the only source of rubber was jungles of South America, the production of rubber was limited and its cost was high until 1890. In 1870, Sir Henry Wickham collected seedlings of Hevea brasiliensis, which was the

most productive source of NR from Brazil, germinated them at Kew Gardens in London, and then started planting them in Ceylon (Sri Lanka), Malay (Malaysia) and lndo-China (Vietnam). By 1920, these countries produced 90 % of the world's supply of rubber. Soon other countries in the region, including the Philippines, Indonesia, Thailand and India became rubber producers. Over the years, production of NR in South America became insignificant but the rubber industry continued to grow with the development of rubber plantations in Asia.

B.F. Goodrich Company patented a new substance in Germany in 1937 that called Chemigum and was the first synthetic rubber (SR). During the Second World War, interruption of the supply of NR created occasion for challenge of developing methods for bulk production of SR in the United States industry. The United States production of GR-S (Government Rubber Styrene also known as the general-purpose styrene-butadiene rubber, SBR, used for tires) was over 700,000 tons in 1945. In I946, the world production of SR had grown to over 900,000 tons while production of NR was about 555,000 tons. The present market share of SR is about 55% out of a grand total of about 15,000,000 tons of both NR and SR [9].

2.2 Rubber

Elastomers are amorphous polymers to which various ingredients are added and this mix is called as compound by rubber chemists [11]. Any elastomer capable of rapid elastic recovery after being stretched to at least twice its length from 0 °F to 150 °F at any humidity [12]. After heating and reaction (vulcanization), these materials become rubber that is one of the most important commercial polymers. In the molecular structure of cured rubber, atoms are connected in long, randomly coil chains that are interlinked at a few points. Between a pair of links each bond can rotate freely regardless of its neighbor. Under stress the molecular chain uncoils and an aligned structure results. After release of the stress the molecules rapidly recover their tangled randomness. This characteristic causes material stretch, less crosslinking density, and an amorphous and non-orientated state, which result in unique properties, such as low hardness, high elasticity, and high elongation break. It swells to more than double its size in organic solvents but is impermeable to water. Vulcanization of rubber creates more sulfide bonds between chains so it makes each free section of chain shorter. The result is that the chains tighten more quickly for a

given length of strain. This increases the elastic force constant and makes rubber harder. Therefore raw rubber is often vulcanized for its applications in the real world [13].

Rubber is a collective term for macromolecular substances of natural origin known as natural rubber (NR) or synthetic origin known as synthetic rubber (SR).

2.2.1 Natural rubbers (NR)

Natural rubber (NR) is a linear, 1,4 addition polymer of isoprene (2-methyl-1,3-butadiene) with a molecular weight of 100,000 to 1,000,000 g/mol. There can be seen *cis*-polymerization of isoprene to form NR in Figure 2.1. It is a free radical polymerization.

Figure 2.1: The *cis*-polymerization of isoprene to form NR [14].

NR is an important strategic raw material for manufacturing a wide variety of industrial products. The source of NR is a milky liquid known as latex which is a suspension containing very small particles of rubber. The liquid latex collection is presented in Figure 2.2.

Figure 2.2: Collection of liquid latex from a rubber tree [15].

There are at least 2,500 different latex-producing plant species; however, only Hevea brasiliensis (the Brazilian rubber tree) is a commercial source [16]. The collected liquid latex is taken to a processing center where the fluid latex is diluted to 15%

rubber content and coagulated with formic acid. The coagulated material is then compressed through rollers to remove water and to produce a sheet material. The sheets are either dried with currents of hot air or by the heat of a smoke fire. The rolled sheets and other types of raw rubber are usually milled between heavy rolls in which the mechanical shearing action breaks up some of the longer polymer chains and reduces their average molecular weight. NR is mixed with small amounts of proteins, lipids, inorganic salts, and numerous other components. The polymer chains of NR are long, entangled, and coiled at room temperature, which are in a state of continued agitation [16].

NR is an elastomer and a thermoplastic. However, it should be noted that as the rubber is vulcanized it will turn into a thermoset. The properties of vulcanized NR is shown in Table 2.1. The tensile strength of NR is increased by vulcanization.

Table 2.1: Properties of vulcanized NR [17].

Property	Numerical value
Tensile strength	17.2 to 24.1 MPa
Elongation at break	750 to 850 %
100% tensile modulus	1.5 MPa
Hardness, Shore A	30-100
Density	0.93 g/cc
Max. usage temperature	82°C
Min. usage temperature	-50°C

NR is one of the most widely used rubbers because of its high flexibility, good elasticity, high tensile strength, electrical insulation property, wear resistance, and good workability. Its comprehensive performance is superior to most synthetic rubbers. On the other hand, it has moderate resistance to environmental damage by heat, light and ozone because of owing to the presence of a double bond in each and every repeat unit [18].

NR forms an excellent barrier to water. This is possibly the best barrier against pathogens, and so latex is used in surgery as surgical and medical examination gloves. It is an excellent spring material. NR latex is also used in catheters, balloons, medical tubes, elastic thread, and also in some adhesives.

2.2.2 Synthetic rubbers (SR)

Synthetic rubber (SR) is a polymer of several hydrocarbons; its basis is monomers such as butadiene, isoprene, and styrene. Almost all monomers for SR are derived from petroleum and petrochemicals. It is a white, crumbly plastic mass which is processed and vulcanized in the same manner as NR [8]. Classification of SR is governed by the International Institute of Synthetic Rubber Producers (IISRP) [19].

The benefits compared with NR include better oil and temperature resistance and the possibility of a product with an extremely constant quality. The mechanical properties are improved by adding fillers such as carbon black (CB) during vulcanization with sulfur. SR is produced in different ways. Figure 2.3 illustrates one of the common production processes.

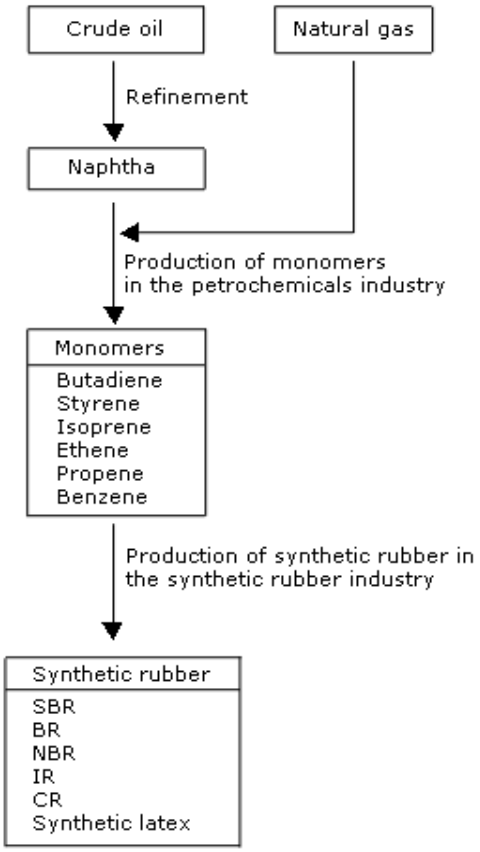

Figure 2.3: Production process of SR [20].

The severe shortages of NR during and immediately after the war stimulated significant research in SR and its technology [8]. Because of volatile or rising prices for NR on the world market in response to the general state of the economy, political events which cut customers off from the suppliers of raw materials, long transport

distances, regional constraints with respect to establishing rubber plantations and the increase in global demand for rubber [20]. According to Malaysian Rubber Board, as can be seen in Figure 2.4, distribution of world rubber consumption results by years shows that SR is more popular than NR.

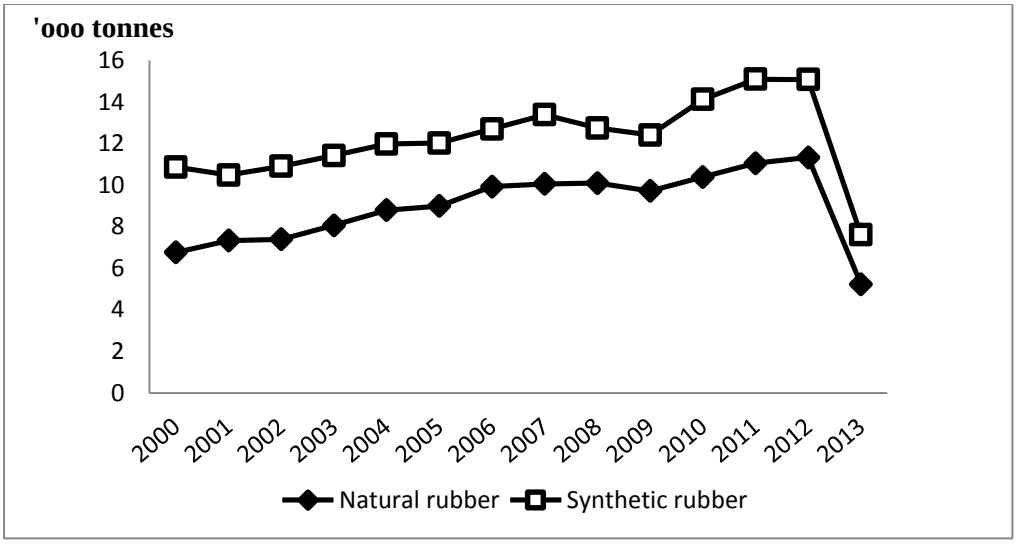

Figure 2.4: World rubber consumption of NR and SR [21].

SRs are further developed than NRs. Examples are synthetic NR, butyl, styrene butadiene, polybutadiene, and ethylene propylene. Styrene-butadiene rubber (SBR) is the most widely used rubber that is explained in section 2.2.2.2. Nitrile rubbers are copolymers of butadiene and acyrolonitrile which are explained in section 2.2.2.6. These rubbers are more costly than ordinary rubbers, so these copolymers are limited to special applications such as fuel hoses and gaskets where high resistance to oils and solvents is required.

2.2.2.1 Polyisoprene (synthetic natural rubber) (IR)

Modern synthetic polyisoprene (IR) is designed to be similar to NR in structure and properties. In 1962, Goodyear company introduced a Ziegler-Natta (titanium-aluminum) catalyzed IR with a cis-1,4 content of 98.5% [12]. Although it still demonstrates lower green strength, slower cure rates, lower hot tear, and lower aged properties than its natural counterpart, IR exceeds the natural types in consistency of product, cure rate, processing, and purity. In addition, it is superior in mixing, extrusion, molding, and calendering processes [22]. This rubber does not require much mastication. Maximum and minimum usage temperatures are approximately 80 °C and -50 °C in air, respectively.

The higher *cis*-1,4 configuration of this polymer closely resembles the properties of natural rubber and is the most important commercially [12]. All the possible chemical structures of IR can be seen in Figure 2.5. The *cis* form is soft and flexible because the chains do not pack well and the overall polymer is mainly amorphous. The *trans* form is hard because the *trans* chains pack well together, able to crystallize due to regular structure.

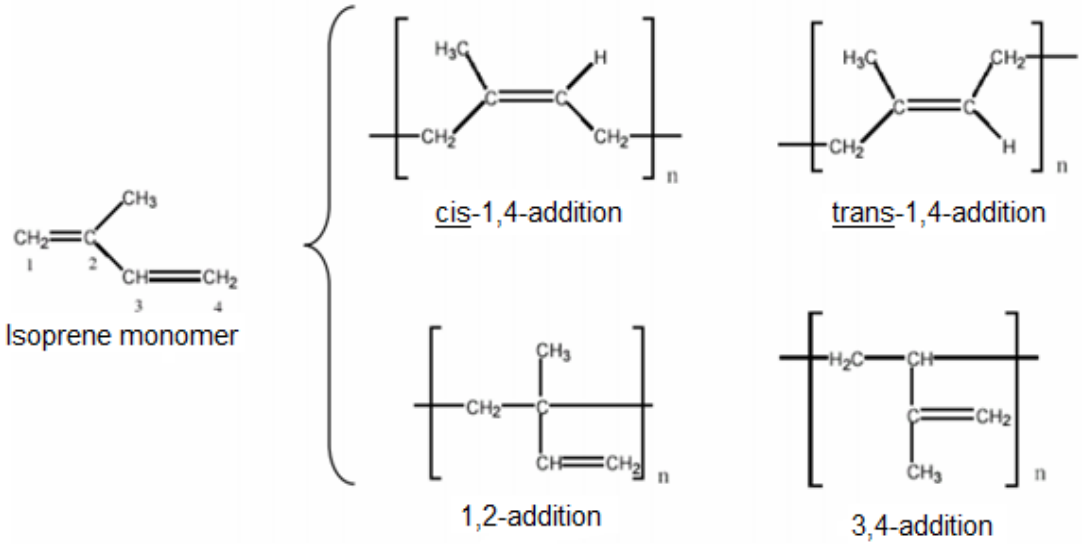

Figure 2.5: Possible chemical configurations of IR [22].

Currently IR is being used in a wide variety of industries in applications requiring low water swell, high gum tensile strength, good resilience, high hot tensile, and good tack. Mineral filled systems find applications in footwear, sponge and sporting goods. In addition, recent concerns about allergic reactions to proteins present in natural rubber have prompted increased usage of the more pure synthetic polyisoprene in some applications.

2.2.2.2 Styrene-butadiene rubber (SBR)

Some of the most commercially important addition polymers are the copolymers. These are polymers made by polymerizing a mixture of two or more monomers. Figure 2.6 presents styrene-butadiene rubber (SBR) which is a random copolymer of 1,3-butadiene and styrene with a styrene content in the range of 10 to 25%.

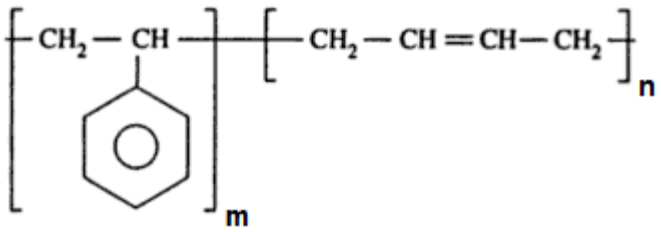

Figure 2.6: Chemical structure of SBR [23].

The presence of styrene contributes to the good wearing and bonding characteristics of SBR and reduces its price. Also, compared with polybutadiene rubber alone, strength, abrasion resistance, and blend compatibility are improved [23]. SBR shows superior wear resistance, heat aging, water resistance, ozone resistance and gas tightness, but its adhesivity, oil resistance and elasticity are not so good compared to the NR [24].

SBR is a synthetic elastomer with wide range of industrial applications. Due to its excellent abrasion resistance and stability it is extensively used as a component of car tires. It is also used for making floor tiles, footwear components, cable insulation.

2.2.2.3 Polybutadiene (BR)

Polybutadiene (BR) is second-largest-volume synthetic elastomer, next only to SBR. BR can be produced by free-radical addition polymerization of butadiene [23]. In addition, it can be polymerization product of 1,3-butadiene monomer in the presence of Ziegler–Natta catalyst system [25]. Chemical structure of BR is shown in Figure 2.7.

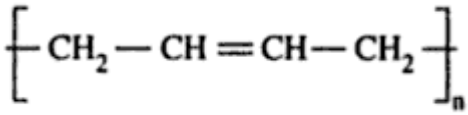

Figure 2.7: Chemical structure of BR [23].

BR provides excellent low temperature flexibility. Like SBR, the principal use of BR is in the production of tires and tire products. BR exhibits good resilience and abrasion resistance and low heat buildup, which are important requirements for tire applications. However, in general, BR processes with more difficulty than SBR.

2.2.2.4 Butyl rubbers (IIR/BIIR/CIIR)

Butyl rubber (isobutylene isoprene rubber, IIR) is a copolymer of isobutylene and isoprene. Chemical structure of IIR is shown is Figure 2.8. Maximum and minimum usage temperatures are about l20°C and -40°C in air. The isoprene content of the copolymer is normally quoted as the 'mole percent unsaturation', and it influences the rate of cure with sulphur, and the resistance of the copolymer to attack by oxygen, ozone and UV light. The polyisobutylene, being saturated, however, naturally confers on the polymer an increased level of resistance to these agencies when compared to natural rubber.

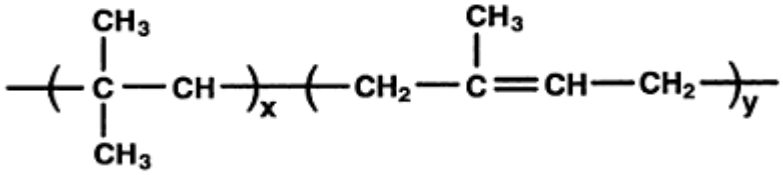

Figure 2.8: Chemical structure of IIR.

Chlorobutyl (CllR) and bromobutyl (BIIR) are modified types containing about 1.1 to 1.3%. wt. of chlorine and bromine, respectively, and the isoprene unit being the site of halogenation [26]. Introduction of the halogen gives greater cure flexibility, and enhanced cure compatibility in blends with other diene rubbers [27]. It also confers increased adhesion to other rubbers and metals.

The main applications of butyl rubbers are in wire and cable applications, inner tubes, inner liners in tubeless tyres, tyre curing bladders, and pharmaceutical closures, the latter utilising the low impermeability of butyl to gases.

2.2.2.5 Polychloroprene (neoprene) (CR)

Polychloroprene (CR) rubbers are homopolymers of chloroprene (chlorobutadiene). Its polymerisation is typically conducted in aqueous emulsion of 2-chlorobutadiene. CR can be compounded for service temperatures of -40°C to 110°C. Chemical structure of CR is illustrated in Figure 2.9.

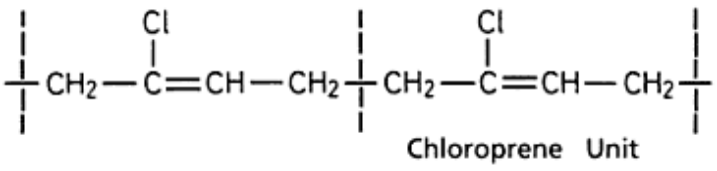

Figure 2.9: Chemical structure of CR.

CR has a well-balanced combination of properties including processability, strength, flexibility, tear resistance, flame resistance, adhesion, weather resistance and ozone resistance for most applications. Typical applications involve power transmission and timing belts, automotive boots, airsprings, and truck engine mounts [9].

2.2.2.6 Nitrile rubber (NBR)

Nitrile rubber (NBR) is a copolymer of butadiene and acrylonitrile (ACN). Chemical structure of NBR can be seen in Figure 2.10. Properties vary with ACN content [28]. The ACN content provides excellent oil and gas permeation resistance [29]. However, an increase in the ACN content causes low temperature flexibility, and increases compound hardness. Typical ACN content ranges from 18% to 50%. Maximum and minimum usages temperatures of NBR are l10°C and -20°C to -40°C (depending upon the grade), respectively.

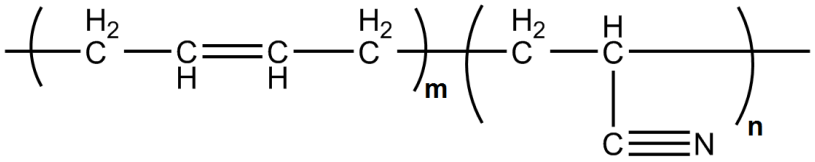

Figure 2.10: Chemical structure of NBR.

Its main applications are in fuel hoses, gaskets, rollers, and other products in which oil resistance is required.

2.2.2.7 Silicone rubbers (Q)

The term ‘silicone’ generally describes polyorganosiloxanes with a main backbone of inorganic siloxane bonds (Si-O-Si) and lateral chains of organic groups. The most common silicones are the polydimethylsiloxanes (MQ) with the structure shown in Figure 2.11. In addition, there can be found also different kinds of Q like silicone rubber with methyl and phenyl substituents (PMQ), silicone rubber with methyl and vinyl substituents (VMQ), as illustrated in Figure 2.11. Substituent groups affect the properties of silicon rubbers, that is presented in Table 2.2.

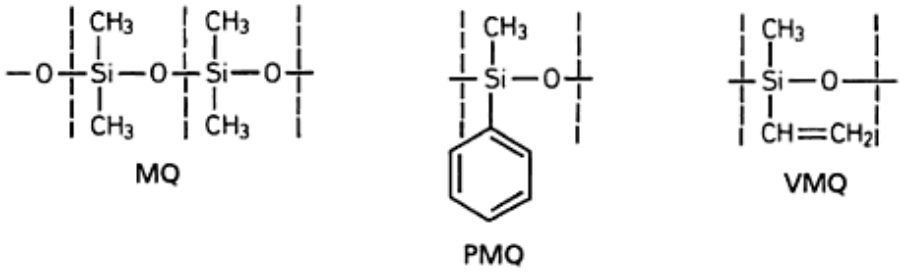

Figure 2.11: Chemical structure of some silicone rubbers [9].

The Si-O-Si bonds in Q have a much lower energy of activation for rotation than C-C bond or C-O bond. This makes Q elastomers flexible and rubbery even at very low temperatures and this elastomeric property is less affected by temperature changes. This feature combined with the refractory characteristics of Q makes these elastomers useful over a wide temperature range.

Q is used in several industrial, automotive, aerospace, electrical-electronics, household, healthcare applications and sporting equipment such as goggles and scuba diving masks, water vapor permeability needed areas [9, 18]. Maximum and minimum operating temperatures of silicon rubbers are about 230°C and -70°C in air. The unique balance of mechanical and chemical properties of silicone rubber have already given it a good position in the market place due to its [9]:

- High temperature resistance,
- Low temperature flexibility,
- Excellent electrical and thermal insulation properties,
- Excellent mechanical properties over a wide range of temperatures, and
- Excellent bio-compatibility and chemical inertness.
- High water vapor permeability

Table 2.2: Effect of substituent groups on properties of silicon rubber [9].

Substituent groups	Acquired quality
CH_3 (Methyl)	General purpose
$CH=CH_2$ (Vinyl)	Network control, strength, high hardness
C_6H_5 (Phenyl)	Extreme low and high temperature resistance, radiation resistance
$CH\text{-}CH_2\text{-}CF_3$	Oil and solvent resistance

2.2.2.8 Ethylene-acrylic rubber (EACM)

Ethylene-acrylic rubber (EACM) is formed from methyl acrylate and ethylene with a carboxylic cure site monomer. It exhibits properties generally comparable to those of an acrylate. The addition of ethylene into the main chain gives low temperature performance [2]. Figure 2.12 illustarates chemical structure of EACM. Maximum and minimum usage temperatures are about l70°C and -40°C, respectively, in air [30]. Chemical resistance is generally poor apart from mineral oils, natural fats and some salts. This is a related material, with excellent high and low temperature resistance, good mechanical strength, good water resistance, good oil resistance and good compression set properties [30].

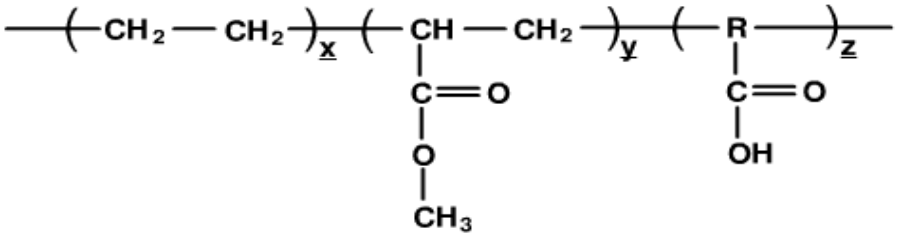

Figure 2.12: Chemical structure of EACM.

This material finds use as a sealing material in automotive applications and marine motor lead wire insulation. It has also been used as the base polymer for low flammability, halogen free, cable jacketing compounds.

2.2.2.9 Ethylene-propylene rubber (EPM/EPDM)

Detailed informations about ethylene-propylene rubbers are explained in Section 2.3.

2.3 EPM/EPDM

Etyhlene-propylene polymers (EPM) are inherently stable rubbery materials, off-white to amber color, and somewhat translucent. Chemical structure of EPM is shown in Figure 2.13. Ethylene-propylene-diene rubber (EPDM) has been the fastest growing elastomer among synthetic rubbers since its introduction in 1963. It represents 7% of the world rubber consumption, and it is the most extensively used in non-tire rubber [31].

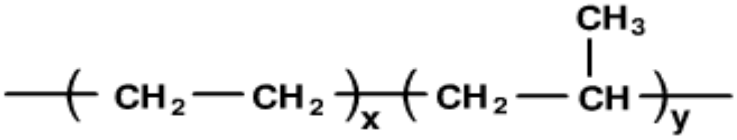

Figure 2.13: Chemical structure of EPM.

2.3.1 Properties of EP(D)M rubbers

The raw EP(D)M rubbers are seldom used alone. Rather, they are compounded with oils, fillers, and curatives and then cross-linked using sulfur- or peroxide-based curing systems. EP(D)M rubbers have a saturated backbone, which explains their excellent weatherability and ozone resistance. EPM polymers have no unsaturation in their structure and therefore, unlike butyl rubber, EPM cannot be vulcanized with sulfur. On the other hand, EPDM polymers have the unsaturation of a termonomer in the side chain of the molecule, permitting direct sulfur cure, as well as chemical modifications. The pendant side-chain can be cleaved by oxygen or ozone, leaving the main chain of the polymer undisturbed [32]. Mechanical, thermal and chemical properties of EP(D)M rubbers are presented in Table 2.3.

By contrast, polymers containing unsaturation in the backbone, such as, butyl (IIR) and natural rubber (NR), are prone to chain breakdown by oxidation or ozone attack, and thus suffer a decrease in molecular weight which alters their mechanical properties with age [3, 33, 34]. Comparison of EPDM rubber properties to other common rubber types is shown in Table 2.4.

Table 2.3: Mechanical, thermal and chemical resistance properties of EP(D)M [35].

Property	ASTM D2000 classification
Mechanical properties (reinforced)	
Hardness, Shore A	35 to 90
Tensile strength (MPa)	4 to 22
Elongation (%)	150 to 800
Tear strength (kN/m)	15 to 50
Thermal properties	
Brittleness point (ºC)	-55 to -65
Min. for continuous service (ºC)	-50
Max. for continuous service (ºC)	150
Chemical resistance	
Weather	Excellent
Ozone	Excellent
Radiation	Excellent
Water	Excellent
Acids and alkalis	Excellent to good
Aliphatic hydrocarbons	Fair to poor
Aromatic hydrocarbons	Fair to poor
Oxygenated solvents	Good

Table 2.4: Comparison of EPDM properties to other common rubber types [35].

Property	Rubber type				
	EPDM	**NR**	**SBR**	**IIR**	**CR**
Specific gravity	0.86	0.92	0.94	0.92	1.23
Tensile strength (max.) (MPa)	22	28	24	21	28
Elongation (%)	500	700	500	700	500
Top operating temp. (ºC)	150 to 175	75 to 120	75 to 120	120 to 180	90 to 150
Brittleness point (ºC)	-55 to -65	-55	-60	-60	-45
Compression set (% in 22 hr at 100 ºC)	10 to 30	10 to 15	15 to 30	15 to 30	15 to 30

2.3.2 EP(D)M characteristics

Although compounding with fillers and other ingredients plays a dominant role in processing and end-use requirements, the characteristics of the base polymer also establish final performances [35]. The principal polymer characteristics of importance are:

- Mooney viscosity (molecular weight)
- Ethylene content
- Diene content
- Molecular weight distribution
- Physical form

The three most important parameters in this aspect are highlighted below.

2.3.2.1 Molecular weight (MW) and Mooney viscosity

This parameter, in combination with molecular weight distribution (MWD), mainly affects rubber processing behavior [3]. Benefits and limitations for EP(D)M, when MW increases, are presented at Table 2.5. Crosslinking of high MW material will be more efficient with the identical amount of curing agent than a low MW material. The same holds for a narrow MWD in comparison with a broad MWD polymer. The former type can be cross-linked more efficiently, due to the absence of a low MW polymer [36]. Mooney viscosity is a bulk viscosity measured in a shearing disk viscometer. There is no simple mathematical relationship between Mooney viscosity and any of the standard MW averages for polymers. This is partly because of the deliberate changes in MWD from polymer to polymer. However, higher Mooney viscosity is a general indication of higher MW of EP(D)M [35].

Table 2.5: Effect of increasing of MW (Mooney viscosity) on EP(D)M [35].

Benefits	Limitations
Tensile and tear strengths increase	More difficult to disperse
Black/oil loading can increase for lower cost	Extrusion rate and ability to calender decrease
Collapse resistance improves	

2.3.2.2 Ratio of ethylene-propylene of EP(D)M

The ethylene-propylene ratio is important factor influencing the results of peroxide cross-linking, as in particular sequential propylene units are inclined to give rise to scission reactions in the presence of reactive peroxides [36]. The crystallisation of EP(D)M is prevented if the ethylene content is in the range 45-60%; higher ethylene contents, 70-80%, can partially crystallise [2]. Thus, high-ethylene EP(D)M can be envisioned as a polyethylene chain with randomly distributed propylene units. In the absence of the methyl groups, the long polyethylene chains associate to form crystalline domains. The presence of the methyl groups reduces the chain packing, which leads to lower crystallinity.

High-ethylene EP(D)M grades have higher tensile and tear strength, increased hardness, improved abrasion resistance, and better heat resistance [32]. High-ethylene EP(D)M grades also have better stability at high temperature due to fewer tertiary hydrogen atoms (from propyl groups), which are prone to attack by radicals. Disadvantages of high ethylene are poor mixing at low temperature and poor low temperature properties. This is because the same ethylene crystalline domains that enhance green strength inhibit a fast recovery after the release of mechanical stresses [3].

2.3.2.3 Choosing of termonomer for EPDM

The copolymerization of ethylene and propylene yields useful copolymers. One disadvantage of the copolymer is that it cannot be cross-linked with sulphur due to the absence of unsaturation in the main chain. To overcome this difficulty a third monomer with unsaturation is introduced, but to maintain the excellent stability of the main chain the unsaturation is made pendant to it. The copolymers can only be cured by peroxides or radiation, whilst the terpolymers can be cured with peroxides, sulphur systems, resin cures and radiation [2].

The three types of third monomer used commercially are dicyclopentadiene (DCPD), ethylidene norbornene (ENB), and l,4-hexadiene (1,4-HD). Chemical structure of these third monomers are illustrated in Figure 2.14.

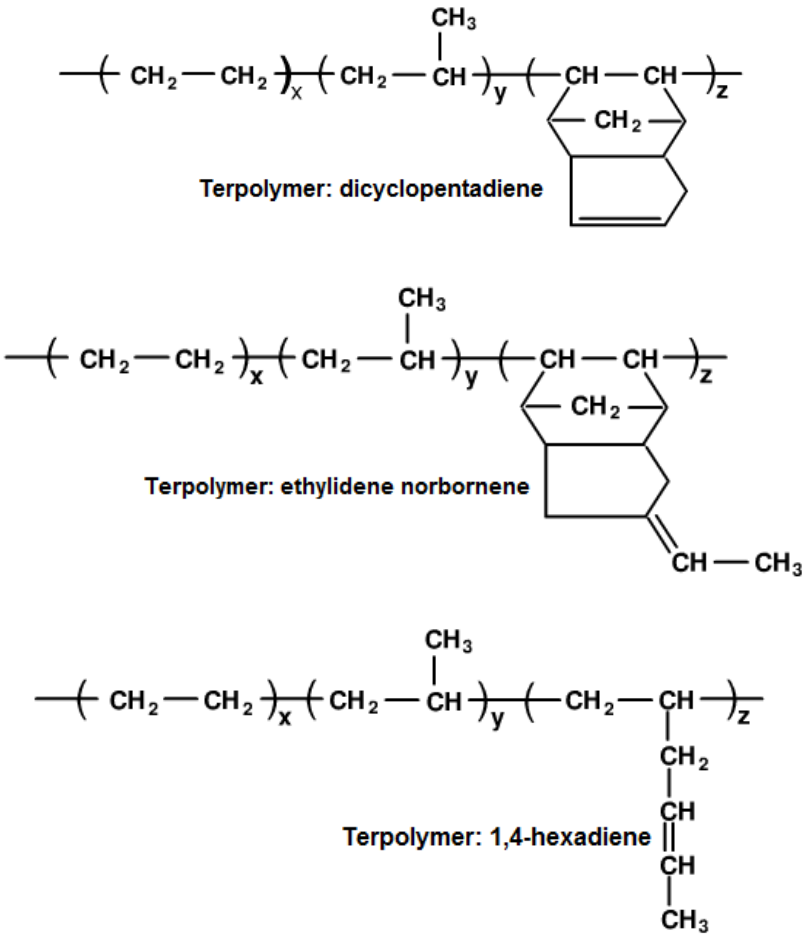

Figure 2.14: Chemical structures of EPDMs with different third monomers [2].

The type of diene used affects the rate at which cross-linking reactions occur during sulfur vulcanization. Generally 4-5% of the termonomer will give acceptable cure characteristics, whilst 10% gives fast cures [2]. The ENB-based EPDM exhibits a much faster cure rate in sulfur vulcanization relative to both DCPD and l,4-HD-based EPDM [3]. DCPD gives the slowest cure rate. An increase in the ENB content of EPDM results good resistance to aging, weathering and chemical resistance, higher modulus, and crosslink density, and as a consequence, a low compression set and better oil resistance in cured EPDM products [1].

2.3.3 Modification of EP(D)M

EP(D)M can be modified with a variety of monomers or inorganic agents.

2.3.3.1 Modification with clays

The mechanical, physical, chemical and tribological properties of EP(D)M depend not only on the molecular weight of the polymer, but also on the reinforcing filler.

The distributions of the filler in the blend and the chemical interactions between EP(D)M and the filler have a significant influence on the performance of the rubber. One of the most widely used fillers is CB, because it improves the stiffness and the toughness of rubber, while maintaining high flexibility and good physical and mechanical properties of the rubber at low manufacturing costs [4].

2.3.3.2 Modification with monomers or inorganic agents

- **Polyproplene and polyethylene**

There are two classes of plastic/rubber blends, TPOs (thermoplastic olefins) and TPEs (thermoplastic elastomers) as defined by Coran. EP(D)Ms are particularly suited for blending with polypropylene (PP) and polyethylene (PE) as TPOs. Brittleness of TPOs which are essentially rigid at the service temperature can be reduced by the addition of EPDM to produce a soft plastic, as illustrated in Figure 2.15, thus increasing their utility.

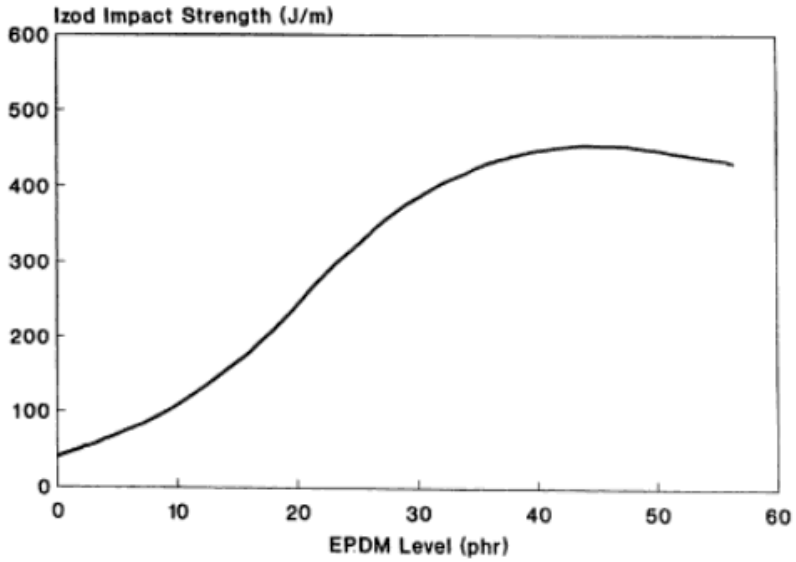

Figure 2.15: Effect of EPDM content on Izod impact strength in PP blends [3].

Their major applications are in automotive industry such as bumper covers, decorative facia, and air ducting [3].

- **Chlorination and bromination**

Chlorination has been heavily realized as a way to impart oil resistance to EPDM. Bromination results faster cure and higher tensile strength of cured EPDM [37].

- **Maleation**

Maleic anhydride modified EPDM (EPDM-g-MA) has found wide use in the lubricants industry for the manufacture of dispersant-grade viscosity modifiers. EPDM-g-MA decreases the activation energy of blends [37].

- **N-vinylpyrrolidone and C-vinylpyridine**

Modification of EPDM with unsaturated pyridines and pyrrolidones are find an application area for production of dispersant-grade viscosity modifiers [37].

- **Antioxidants**

EPDM which one based on ethylidene norbornene (ENB) is very sensitive to thermal oxidation because of its structure . Thermo-oxidative aging of EPDM initially results chain scissions of EPDM molecular chains, and thus the formation of large number of free radicals that attack the double bonds of EPDM chains and cause decrement of crosslinking density. Therefore, it is necessary to add some antioxidants to improve thermo-oxidative aging resistance of EPDM for the applications at high temperature, especially for EPDM with high ENB content [34]. In addition, grafting antioxidants onto EPDM provides a nonmigrating, nonextractable antioxidant for lubricant applications and applications in contact with fluids [37].

- **Styrene-acrylonitrile**

Styrene-acrylonitrile grafts on EPDM are used for weather resistant applications and plastics impact modification.

2.3.4 EP(D)M applications

Wire and cable applications, window seals and car door seals, roofing membranes, gaskets, hose and tubing, tire sidewalls and footwear [38]. As an example of the considerations to be made when formulating with EPDM, a generic formulation for an automotive radiator hose is shown in Table 2.6.

Table 2.6: Generic formulation for an automotive radiator hose [3].

Chemical	phr
EPDM	100
CB	150
Calcium carbonate	80
Paraffinic oil	120
Zinc oxide	3
Stearic acid	2
Sulfur	1.5
MBT	1.5
TMTD	1.0
DPTS	0.5

These non-polar rubbers are used in applications where NR has a short life. Washing machine door seals molded from EPDM are starting to replace NR. They are also used in applications with fire retardant hydraulic fluids (phosphate ester type), many aqueous solutions, acids, alkalis, alcohols and silicone oils. They can also be used in systems handling potable water and water-based materials [30].

2.4. Compounding and Vulcanisation of Synthetic Rubbers

Compounding, a term that has evolved within the tire and rubber industry, is the materials science of modifying a rubber or elastomer or a blend of polymers with a series of additives to optimize properties to meet a given service application or set of performance parameters [19]. The choice of the base polymer and the additives is closely linked to the type of properties to be achieved. The resulting product is a non-vulcanized compound [39].

The ingredients which are used for formulating a rubber compound can be divided into five categories: polymers (NR, synthetic polymers) , filler systems (CB, clays, silicas, calcium carbonate), stabilizer systems (antioxidants, antiozonants, waxes), vulcanization system components (sulphur, peroxide, accelerators, activators) and special materials (secondary components such as pigments, oils, resins, processing aids, and short fibers) [40]. In Table 2.7, an example for material-compound type is presented.

Table 2.7: Conveyor belt cover compound [40].

Material	phr	Compound type
NR	100.0	Elastomer
N 220 CB	45.0	Black reinforcer
ZnO	4.0	Activator
Stearic acid	2.0	Activator
Rubber process	4.0	Softener
Agerite resin D	2.5	Age resister
Paraffin wax	1.0	Age resister
CBS	0.5	Accelerator
Sulfur	2.5	Vulcanizing agent

2.4.1 Vulcanization system

Vulcanization, named after Vulcan, the Roman God of Fire, describes the process by which physically soft, compounded rubber materials are converted into high-quality engineering products [40, 41]. The vulcanization system constitutes the fourth component in an elastomeric formulation and functions by inserting cross-links between adjacent polymer chains in the compound. A typical vulcanization system in a compound consists of three components: activators, vulcanizing agents, accelerators and retarders-antireversion agents.

2.4.1.1 Vulcanizing agents

Vulcanizing agents are necessary for the crosslink formation. These vulcanizing agents are mostly sulphur or peroxide and sometimes other special vulcanizing agents or high energy radiation [40, 42]. Since vulcanization is the process of converting the gum-elastic raw material into the rubber-elastic end product, the ultimate properties like hardness and elasticity depend on the course of the vulcanization [39].

Three vulcanizing agents find extensive use in the rubber industry: sulfur, insoluble sulfur and peroxides.

Sulfur is soluble in natural rubber at levels up to 2.0 phr. Above this concentration, insoluble sulfur must be used to prevent migration of sulfur to the compound surface,

i.e., sulfur bloom. Peroxide does not enter into the polymer chains but produces radicals that form C-to-C linkages with adjacent polymer chains.

2.4.1.2 Activators

The vulcanization activator system consist of zinc oxide and stearic acid. They activate the vulcanisation process and help the accelerators to achieve their full potential. Stearic acid and zinc oxide levels of 2.0 and 5.0 phr, respectively [40].

2.4.1.3 Accelerators

Accelerators are products which increase both the rate of sulfur crosslinking in a rubber compound and crosslink density. On the other hand these agents lower the sulphur content necessary to achieve optimum vulcanizate properties [43]. Secondary accelerators, when added to primary accelerators, increase the rate of vulcanization and degree of crosslinking. Mercaptobenz-thiazole (MBT), N-cyclohexylbenz-thiazylsulfenamide (CBS) and sodium diethyl dithiocarbamate (SDC), tetramethyl thiuram disulfide (TMT, TMTD) can be given as examples for primary and secondary aaccelerators, respectively.

2.4.1.4 Retarders and antireversion agents

The induction time or scorch resistance of a compound can be improved by addition of a retarder. N-Cyclohexylthiophthalimide (CTP) is by far the largest-tonnage retarder used in the rubber industry [40].

2.4.2 Filler system

Fillers, or reinforcement aids, such as CB, clays, and silicas are added to rubber formulations to meet material property targets such as tensile strength and abrasion resistance. There are two types of fillers, reinforcing and non-reinforcing fillers. CB is commonly used as reinforcing filler [40]. This is also the reason why most rubbers are black. Calcium carbonate is an example of a non-reinforcing filler [44].

2.4.3 Stabilizer system

The unsaturated nature of an elastomer accounts for its unique viscoelastic properties. However, the presence of carbon-carbon double bonds renders elastomers

susceptible to attack by oxygen, ozone, and also thermal degradation. These agents increase the resistance to attacks of ozone, UV light and oxygen.

2.4.4 Special compounding ingredients

In addition to the four primary components in a rubber formulation, there are a range of secondary materials:

- Processing oils (aromatic oils, naphthenic oils, paraffinic oils): Chemicals that improve the processability [40].
- Plasticizers: Besides fillers, plasticizers play the biggest quantitative role in building a rubber compound. The reasons for the use of plasticizers are improvement of flow of the rubber during processing, improved filler dispersion, influence on the physical properties of the vulcanizate at low temperatures. Mineral oils and paraffins are widely used as a plasticizer.
- Resins, and coloring agents (e.g., titanium dioxide used in tire white sidewalls): Organic and inorganic pigments are used to colour rubber compounds. The colour pigments are also considered inactive fillers. Only silicas have a reinforcing effect. Silicone can be coloured easily without loss of properties [40].

2.5 Rubber Mixing Systems

In the early history of rubber compounding, it was found that softening the elastomer was useful that is basis of mixing the elastomer to make it receptive to other ingredients. Most common types of mixing equipment: two-roll mills, internal batch, mixers and continuous mixers.

2.5.1 Two-roll mill

In many cases, the two-roll lab mill is a device that is used for preparing small quantities of mixed compound by the rubber technologist. This mixing device is usually set for a ratio of roll surface frictional speed of about 1.25: 1 [45]. The two-roll lab mill is illustrated in Figure 2.16. According to the Figure 2.16, numbers on shape is explained in Table 2.8. Two-roll mill parameters are roll speed, speed ratio or friction ratio, nip gap, roll diameter and length [46].

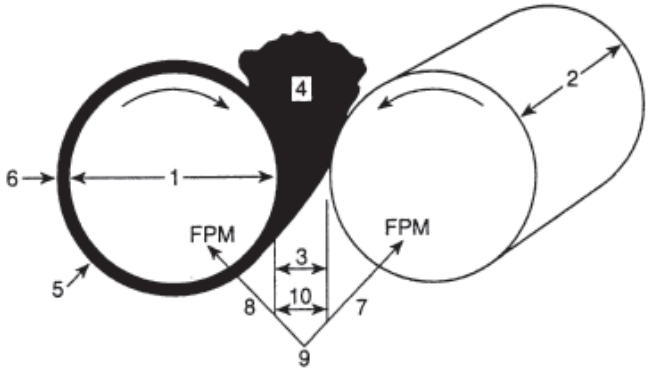

Figure 2.16: Two-roll mill.

Table 2.8: Explanation of parts of two-roll mill [45].

Nomenclature	Explanation
1. Diameter (D)	Usually same for both rolls
2. Face length (L)	Roll length (mill sizes expressed as DxL)
3. Roll gap	Distance between rolls
4. Bank size	Material sitting above gap
5. Banded roll	Roll which material follows
6. Front roll	Roll on operator's side
7. Slow roll	Roll rotating at slowest speed
8. Fast roll	Roll rotating at fastest speed
9. Friction ratio	Roll speed ratio
10. Separating force	Resultant force exerted by material in roll gap

The rolls can be heated or cooled as necessary. The rubber is placed on the rolls and additives are added in carefully weighed quantities during the mixing process. After the mixing operation is complete, the compound is removed from the mill in the form of sheet. The disadvantages of mill mixing may be listed as follows:

1. Length of the mixing cycles
2. Dependence on operator skills
3. Dust and dirt levels that are typical

4. Difficulty in standardizing subjective procedures
5. Difficulty in controlling batch-to-batch uniformity

2.5.2 Internal batch mixers

In large rubber factories, especially tire factories, the internal batch mixer has practically replaced the two-roll mill for the preparation of compounds. With internal batch mixers, an operator only performs charging and discharging whereas with the two-roll mill, the whole mixing operation is carried out by the operator. In contrast to the mill, more uniform compounds and large batches can generally be prepared by the internal batch mixer. In addition to these advantages, the internal batch mixer is faster, eliminates dust and fumes hazards, uses less floor space [45]. The principal components of an internal batch mixer is shown in Figure 2.17.

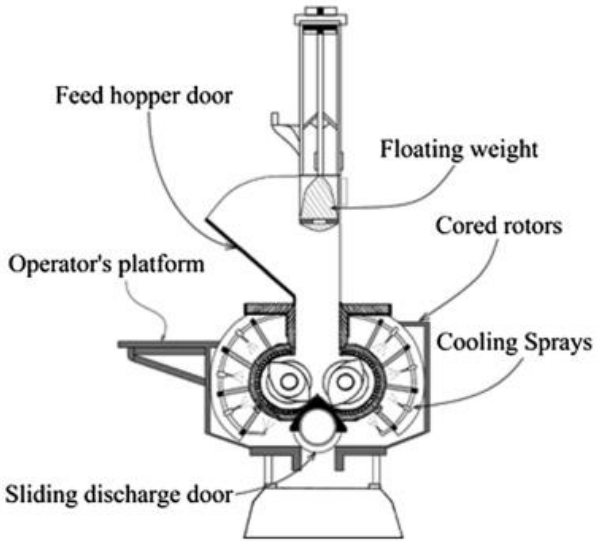

Figure 2.17: Internal batch mixer [45].

The internal batch mixers are made in two basic types of rotors: non-intermeshing also called tangential type (the Banbury mixer) and intermeshing type (the Internal mixer).

2.5.2.1 Banbury mixers

The Banbury mixer has a double partitioned kneader that has two adjacency cylindrical sections which meet tangentially [47]. The material is obtained from the mouth of the feeding hopper into a tapering nip between the rotor wings and chamber sidewall by the rotor clipped to provide the compression and shear and the transfer of

material around the mixing chamber from one rotor to the other in order to provide dispersion as shown in Figure 2.18.

Figure 2.18: Pathlines of non-intermeshing rotors [45].

2.5.2.2 Internal mixers

Intermeshing rotor machines have tended to be larger, and more expensive, for a particular mixing batch size because of the larger relative diameter of an intemeshing rotor to the mixing volume available. Intermeshing rotors rotate at the same speed and the mixing effect is achieved as in a tangential system, but with this system mixing also takes place in the nip between the rotors. Compared to the tangential intermeshing system this system has more effective temperature control, lower viscosity products, drive power is higher but optimum fill levels are lower because of the narrow intermeshing zone [48].

2.5.3. Continuous mixers

Because of the numerous compounding ingredients used in the rubber industry and their varying physical form, it is difficult to achieve an economic and sufficiently accurate proportioning of the compounds in a continuously operating machine. Rubber extruders are machines that force material through a die or nozzle to give a profile strip. They fall into two types: those in which the pressure is produced by a ram and those in which it is produced by a screw. The screw extruder is the type most often used in the rubber industry which has two type as single-screw extrusion and twin-screw extrusion; the ram extruder is a more specialized machine for short runs [45]. A diagram of screw extruder is shown in Figure 2.19.

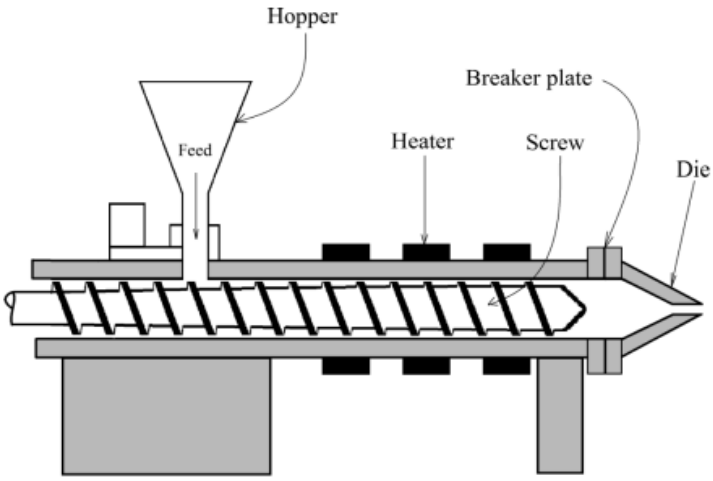

Figure 2.19: Diagram of screw extruder [45].

2.6 Nanocomposites

A composite is a combination of two or more different materials that are mixed in an effort to blend the best properties of both. A nanocomposite is a composite material, in which one of the components has at least one dimension that is nanoscopic in size, that is around 10^{-9} m [49]. The introduction of inorganic nanoparticles as additives into polymer systems has resulted in polymer nanocomposites (PNCs) exhibiting multifunctional, high performance polymer characteristics beyond what traditional filled polymeric materials possess [5]. PNCs consist of a polymeric material (e.g., thermoplastics, thermosets, or elastomers) and a reinforcing nanoparticle. PNCs show major improvements in mechanical properties, gas barrier properties, thermal stability, fire retardancy, and other areas. Table 2.9 presents several benefits and disadvantages when nanoparticles are incorporated into the polymer matrix.

Many factors affect the polymer nanocomposite properties [50]:

- Synthesis methods such as melt compounding, solvent blending, in-situ polymerization, and emulsion polymerization,
- PNC morphology,
- Types of nanoparticles and their surface treatments,
- Polymer matrix such as crystallinity, molecular weight, polymer chemistry, and whether thermoplastic or thermosetting.

Table 2.9: Effect of nanoparticles on the polymers [50].

Improved properties	Disadvantages
• Mechanical properties (tensile strength, stiffness, toughness) • Gas barrier • Synergistic flame retardant additive • Dimensional stability • Thermal expansion • Thermal conductivity • Abrasion resistance • Chemical resistance • Reinforcement	• Viscosity increase (limits processability) • Dispersion difficulties • Optical issues • Sedimentation • Black color when different carbon containing nanoparticles are used

Depending on the application, the type of nanoparticle needed to provide the desired effect must be determined. Some of the most commonly used nanoparticles are montmorillonite organoclays (MMT), carbon nanofibers (CNFs), polyhedral oligomeric silsesquioxane (POSS), carbon nanotubes CNTs, nanosilica (N-silica), nanoaluminum oxide ($A1_2O_3$), nanotitanium oxide (TiO_2), halloysite nanotubes (HNTs), etc.

2.7 Halloysite Nanotubes (HNTs)

2.7.1 Chemical structure of HNTs

Naturally formed halloysite is a kind of aluminosilicate clay ($Al_2Si_2O_5(OH)_4.nH_2O$ with 1:1 layer) with hollow micro and nanotubular structure, and are mined from natural deposits in countries like China, New Zealand, America, Brazil, and France. HNTs are chemically similar to kaolinite [7]. HNTs contain two types of hydroxyl groups, inner and outer hydroxyl groups, which are situated between layers and on the surface of the nanotubes, respectively. The surface of HNTs is mainly composed of the siloxane surface [6]. Figure 2.20 shows schematic structure of a halloysite nanotube. HNTs are ultra-tiny hollow tubes with diameters typically smaller than

100 nanometres (nm) , with lengths typically ranging from about 500 nm to over 1.2 microns [51].

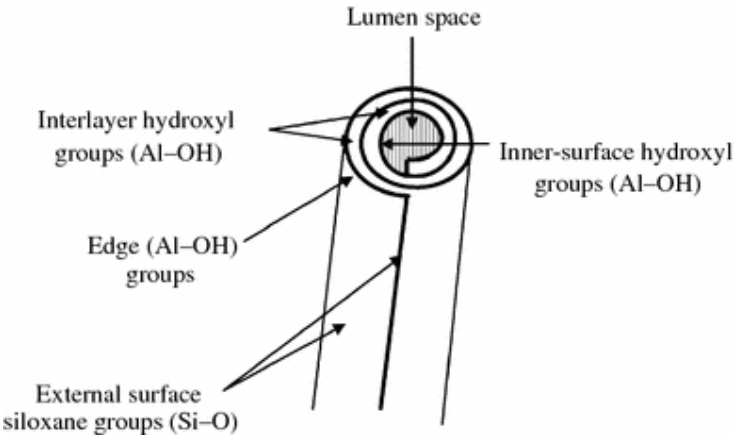

Figure 2.20: Schematic structure of a halloysite nanotube [51].

2.7.2 Advantages of HNTs

Green nanotechnology aims at developing environment safe and less harmful nano products. Because halloysite is non-toxic, biocompatible and EPA 4A listed material, halloysite clay nanotubes, nanocomposites, nano powders, etc. are now emerging as trendsetters in green nanotechnology. In recent years, there has been growing concern about the effect of carbon nanotubes on human health and on environment because of their potential toxic nature. Various features of HNTs like rigidity, higher aspect ratio, and easy dispersibility in polymer matrix and more importantly its abundant availability and biocompatibility make it a subject of fascination. In addition, HNTs reduce the volume of costly active agents.

2.8 Literature Review

In literature, there can be found various studies about HNTs filled nanocomposites or specifically HNTs filled EPDM nanocomposites. Some of the important studies from literature are given in chronological order at below.

Ismail and co-workers studied on morphological, thermal and tensile properties of HNT filled EPDM nanocomposites. HNTs with from 0 to 100 phr were added to EPDM rubber samples and mixed on two-roll mill. According to the morphological study of the fractured surfaces of EPDM/HNT nanocomposites, the dispersion of HNTs inside the EPDM matrix was observed homogenous. In addition, the interfacial and inter-tubular interactions between HNTs and EPDM were quite good.

As a result, tensile strength, elongation at break, tensile modulus at 100% elongation (M100) and crosslink of EPDM/HNTs nanocomposites showed significant increase, especially at high HNTs loading [52]. After that study, Ismail et. al. concentrated on curing behavior of HNT filled EPDM nanocomposites. EPDM/HNT nanocomposites were prepared by mixing 0 to 100 phr of HNTs with EPDM on a two-roll mill. Ismail and co-workers investigated that tensile properties were increased of EPDM nanocomposites with the mixing HNTs with EPDM. The scorch time and cure time (t_{90}) decreased with increasing HNT loading (up to 15 phr). However, penetration of EPDM in to the tubular structure of HNTs at HNT loading higher than 15 phr, resulted delay the curing of composites. On the other hand, cure time was still lower than the cure time of pure EPDM without HNT. A good adhesion between HNTs with EPDM matrix was observed by SEM micrographs. It was proved that HNT could be a novel nano-filler for enhancing the mechanical properties of EPDM, because of its nano-sized dimensions, and easily processed characteristics [53]. Ismail et al. also studied on the effects of palm ash (PA)/halloysite nanotubes (HNTs) weight ratio on the curing characteristics, tensile properties and morphology of the hybrid composites. PA/HNTs/EPDM hybrid composites were prepared by incorporation of hybrid nanotubes into EPDM rubber matrix on a laboratory size two-roll mill. The increase of HNTs in the weight ratio of PA/HNTs increases the scorch time, cure time, maximum torque, tensile strength and tensile modulus (M100 and M300) of PA/HNTs/EPDM hybrid composites but decreases the elongation at break. Morphological studies of tensile fracture surfaces of PA/HNTs/EPDM hybrid composites indicated that HNTs has better adhesion to the EPDM matrix as compared to palm ash [54].

Pasbakhsh and co-workers examined effect of partial replacement of silica or calcium carbonate (CaCO3) by HNTs on the thermal, mechanical and morphological characteristics of EPDM composites. EPDM/Silica/HNT and EPDM/CaCO3/HNT compositions (i.e. 100/30/0, 100/25/5, 100/15/15, 100/5/25, and 100/0/30 phr) were prepared on a two-roll mill. The results showed that the mechanical properties of CaCO3 by HNTs continuously increased with increasing of HNT from 0 to 30 phr loading, while the optimum values of tensile properties were obtained for 100/25/5 phr composition of EPDM/Silica/HNT. In addition, according to SEM investigations co-incorporation of 5 phr of HNTs with silica would improve the dispersion of silica

and enhanced the interactions between silica and EPDM matrix. Therefore, it was clear to say that HNTs could be used as a co-filler to obtain better dispersion of silica inside the EPDM. As a result of replacement of silica or CaCO3 by HNTs, the cure time (t_{90}) and cure rate were decreased and increased, respectively [55]. In their next study, the effect of maleic anhydride grafted EPDM (MAH-g-EPDM) compatibilizer on the interactions, and tensile and morphological properties of HNTs filled EPDM nanocomposites was investigated. MAH-g-EPDM has been successfully prepared by melt compounding of the EPDM, maleic anhydride and DCP. The tensile properties of the nanocomposites were influenced by hydrogen bonding between MAH-g-EPDM and HNTs that caused the creation of an interphase between EPDM and HNT by MAH-g-EPDM that helps to make stronger interfacial interactions. It was found that the presence of these compatibilizers reduced the curing time (t_{90}) but increased the maximum and minimum torques. XRD patterns indicated that the degree of intercalation of the HNTs inside the compatibilized EPDM/HNT nanocomposites is much higher than the uncompatibilized nanocomposites [56]. For other study, Pasbakhsh and co-workers presented effects of modification of HNT on EPDM/HNT nanocomposites. Modification process of HNT was made with γ-methacryloxypropyl trimethoxysilane (MPS) to improve their dispersion in EPDM. The tensile strength and tensile modulus at 100% elongation (M100) of the nanocomposites were higher than those of EPDM/unmodified HNTs while the elongation at break decreased a little after modification of the HNTs. SEM and TEM studies revealed the better dispersion of the modified HNTs in the EPDM matrix. FTIR and TGA indicated that γ-MPS had partially penetrated into the HNTs and interacted with the Si–O groups on the surfaces of the HNTs [57]. In addition, Pasbakhsh et. al. studied on electron beam irradiation of sulphur vulcanized EPDM nanocomposites reinforced by HNTs. EPDM/HNTs nanocomposites were prepared with 0, 10, 30 and 100 phr HNTs addition to EPDM matrix in the presence of sulphurating agents. The EB irradiation dosages of 0, 50, 100 and 150 kGy were applied on the EPDM/HNTs nanocomposites. The enhanced mechanical properties of irradiated EPDM/HNTs nanocomposites were investigated up to 30 phr HNTs loading due to the better dispersion of HNTs within the EPDM after applying EB irradiation. The tensile strength of the EPDM/HNT nanocomposites at low (up to30 phr) and high (100 phr) HNT loadings increased and decreased respectively. The elongation at break decreased after applying EB irradiation [58].

Guo et. al. worked on sorbic acid (SA) modified SBR/HNTs nanocomposites. SA was used to improve the performance of SBR/HNTs nanocomposites by direct blending. The strong interfacial bonding between HNTs and SBR matrix is resulted through SA intermediate linkages. The interactions between HNTs and SA provided that dispersion of HNTs significantly improved. Promised mechanical properties of SA modified SBR/HNTs nanocomposites were obtained by the interactions between HNTs and SA and improved dispersion of HNTs [59]. On the other hand, Raman and co-workers examined the effect of HNTs on solution SBR (SSBR). Because of being highly hydrophilic, HNTs were modified by different silane coupling agents to provide good dispersion in hydrophobic SSBR matrix. According to tensile test results, modified HNTs filled SSBR nanocomposites had higher tensile strength and elongation at break than unmodified HNT filled nanocomposites. Transmission electron microscopic analysis showed that the dispersion of modified HNTs had better dispersion than unmodified HNTs in SSBR matrix. Thermal stability of SSBR nanocomposites is increased marginally in the presence of silane functionalized HNTs [60].

Rooj et. al. aimed to work on a green composite, and they studied on naturally occurring HNTs and NR. A silane coupling agent, bis (triethoxysilylpropyl)-tetrasulphide, was used to enhance the properties of NR/HNT composites. They investigated that reinforcement property of HNTs was better than commercial silica coupled with the same amount of silane coupling agent, because of observing the higher physical properties of the composites filled with HNTs.TEM images revealed that dispersion of the HNTs was good in the rubber matrix [61]. Ismail and co-workers compared the properties of HNTs filled standard Malaysian rubber (SMR L) and epoxidized natural rubber (ENR 50). Scorch times (ts_2) and cure times (t_{90}), tensile modulus values (M100 and M300), and thermal stabilities of both SMR L/HNTs and ENR 50/HNTs nanocomposites increase with the addition of HNTs. Tensile strengths of both nanocomposites increased up to 20 phr HNTs loading, after that point tensile strengths started to decrease. While HNTs loading increased, elongations at break, swelling percentages, and fatigue lifes of nanocomposites showed decrease. Ismail et. al. investigated that ENR 50 nanocomposites had shorter scorch time, longer cure time, and slower curing rate index with higher maximum torque than SMR L nanocomposites. Moreover, ENR 50 nanocomposites had higher

M100 and M300 and thermal stability with lower swelling percentage than SMR L nanocomposites. However, SMR L nanocomposites showed better performance for tensile strength, elongation at break, and fatigue life. Due to SEM micrographs, nanocomposites and HNTs had better interaction and dispersibility at lower filler loading [62]. Ismail et. al. also worked on properties of HNT filled NR by using two different mixing methods, i.e., mechanical and solution mixing. The result showed that the addition of HNTs caused increase in scorch time, cure time and maximum torque for both mechanical mixing and solution mixing methods. However, nanocomposites which prepared via solution mixing had longer scorch and cure time than nanocomposites prepared via mechanical mixing method. SEM showed that nanocomposites prepared via solution mixing method had better dispersion of HNTs than nanocomposites prepared via mechanical mixing method. Inclusion of HNTs caused a reduction in swelling percentage, fatigue life but increased the thermal stability of both nanocomposites [63].

Ye and co-workers worked on to mix HNTs incorporated epoxy resin and carbon fibre textiles to obtain epoxy/HNT/carbon fibre multi-scale composites. Addition of HNTs improved both the storage modulus and T_g of the composites. These results proved a synergistic effect between HNT and carbon fibres [64].

Soheilmoghaddama and co-workers investigated structural, morphological, thermal and mechanical properties of regenerated cellulose (RC)/HNT nanocomposites. At 6 wt.% HNT film, tensile strength and tensile modulus of RC films improved by 55.3% and 100%, respectively. Addition of HNT to the RC reduced moisture absorption of an environment with 75% constant relative humidity. The presence of HNT enhanced the thermal stability and char yield of RC. The significant reinforcing effects of HNTs demonstrated that there was a possible interface interaction between cellulose and HNT which yielded better thermal and mechanical properties of the nanocomposite films as compared to pure RC [65].

3. EXPERIMENTAL

3.1 Materials

3.1.1 Ethylene propylene diene monomer (EPDM)

Two kinds of EPDM, Keltan 778Z with ethylene content of 67%, ENB of 4.3% and M_L (1+4) at 125 °C of 63 MU; Keltan 6950 with ethylene content of 48%, ENB of 9% and M_L (1+4) at 125 °C of 65 MU, were used as the matrix in this work. They were supplied by Arsan Kauçuk Plastik-Makina Sanayi ve Ticaret A.Ş., Turkey.

3.1.2 Halloysite nanotubes (HNTs)

The HNTs (ultrafine grade) were contributed by Eczacıbaşı Esan Endüstriyel Ham Madde Sanayi ve Ticaret A.Ş., Turkey. The elemental composition of HNTs was as follows: (wt. %) SiO_2, 43.3; Al_2O_3, 38.4; Fe_2O_3, 0.8; TiO_2, 0.1; CaO, 0.08; MgO, 0.12; Na_2O, 0.27; K_2O, 0.12. It was used as a reinforcement agent.

3.1.3 Di (tert-butylperoxyisopropyl) benzene (Perkadox 14-40B)

Perkadox 14-40B was obtained from BUR-KIM Kauçuk ve Kauçuk Kimyasalları Ltd. Şti., Turkey**.** It was used on the purpose of curing of components.

3.1.4 Zinc oxide (ZnO)

ZnO was contributed by Arsan Kauçuk Plastik-Makina Sanayi ve Ticaret A.Ş., Turkey. It was used as a stabilizer for high temperatures of the compound.

3.1.5 Stearic acid

Stearic acid was obtained from Arsan Kauçuk Plastik-Makina Sanayi ve Ticaret A.Ş., Turkey. It was used as a processing aid for curing.

3.1.6 Triallyl cyanurate (Rhenofit TAC)

Rhenofit TAC was supplied by RPM Prod, Turkey. It was used as an activator for Perkadox 14-40B.

3.2 Equipments

3.2.1 Equipments used for preparation of rubber compound

3.2.1.1 Two-roll mill

Laboratory type 8" diameter, 16" wide chromed two-roll mill (open mill) with 1.25:1 friction ratio was used to prepare EPDM/HNTs nanocomposites and EPDM compounds. The used two-roll mill is shown at Figure 3.1.

Figure 3.1: Industrial type two-roll mill while it was working. (photo by Polat Yağmur, 2013.)

3.2.2 Equipments used for unvulcanized compound

3.2.2.1 Density measuring instrument

The density of compounds was measured according to ISO 2781.

3.2.2.2 Mooney viscometer (MV)

The effects of temperature and time on the viscosity of rubbers were measured by the Mooney viscometer (MV, MonTech MV 3000 Basic) at 100 °C according to ASTM D 1646. The used MV is shown at Figure 3.2.

Figure 3.2: Mooney viscometer. (photo by Polat Yağmur, 2013.)

Dr. Melvin Mooney designed viscometer that consists of a disk rotating inside a cylindrical cavity formed by two dies maintained at specific conditions of temperature and die closure force [11]. The rotating disk is embedded in a rubber specimen to measure the viscosity of raw rubbers, as well as rubber compounds with additives [9]. The working principle of a rotating disk of viscometer is shown at Figure 3.3.

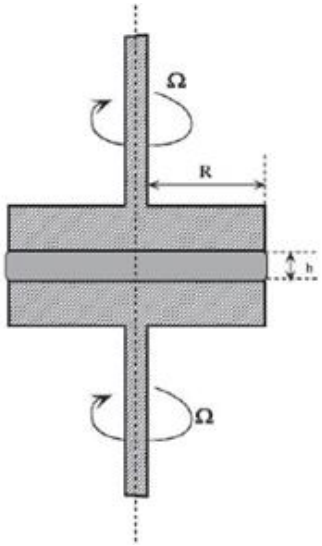

Figure 3.3: Schema of rotating disk of viscometer [9].

Before and during MV test, the following conditions must be considered:

1. Rubber situation: Milled or unmilled.
2. Test temperature.
3. Preheating time.

4. Test running time
5. Size of rotor.

The standard test temperature for Mooney is usually 100°C. The most common test condition is to specify preheating time and running time as M_L (1 + 4). M_L (1 + 4) presents measurement of Mooney viscosity: Preheating without rotation of the rotor and running time with rotation, respectively 1 min and 4 min. The MV curve can be seen at Figure 3.4.

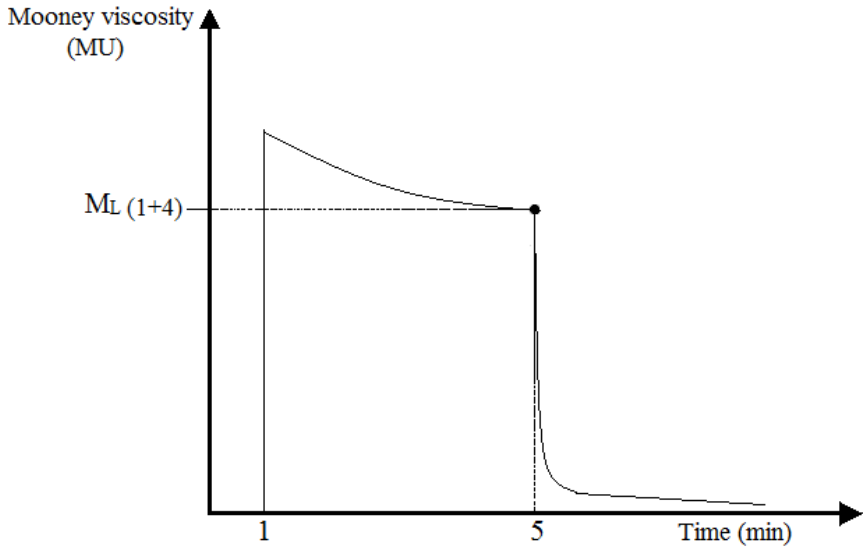

Figure 3.4: Schema of typical Mooney viscosity curve [66].

3.2.2.3 Moving die rheometer (MDR)

Rheological behavior of uncured rubber was investigated with moving die rheometer (MDR, MonTech MDR 3000 Basic) at 192 °C. Rheometer was used according to ASTM D5289 is shown at Figure 3.5.

Figure 3.5: Moving die rheometer. (photo by Polat Yağmur, 2013.)

The MDR measures cure properties and changes in stiffness under isothermal test conditions with constant strain and frequency of uncured rubber compound. Cure properties are measured by the increase in the torque required to maintain a given amplitude of oscillation at a given temperature. The torque is proportional to low strain modulus of elasticity. The torque is plotted against time to give a so-called cure curve. The uncured compound sample is compressed between two heated platens by an applied oscillating force. The MDR applies a sinusoidal strain to the rubber specimen by oscillating the lower die. The reaction torque transducer is attached to the upper die and separated from the lower oscillating die. This separation produces a signal that gives information about the property of the rubber [19]. As can be seen below typical aspect of cure curve of compound is shown at Figure 3.6.

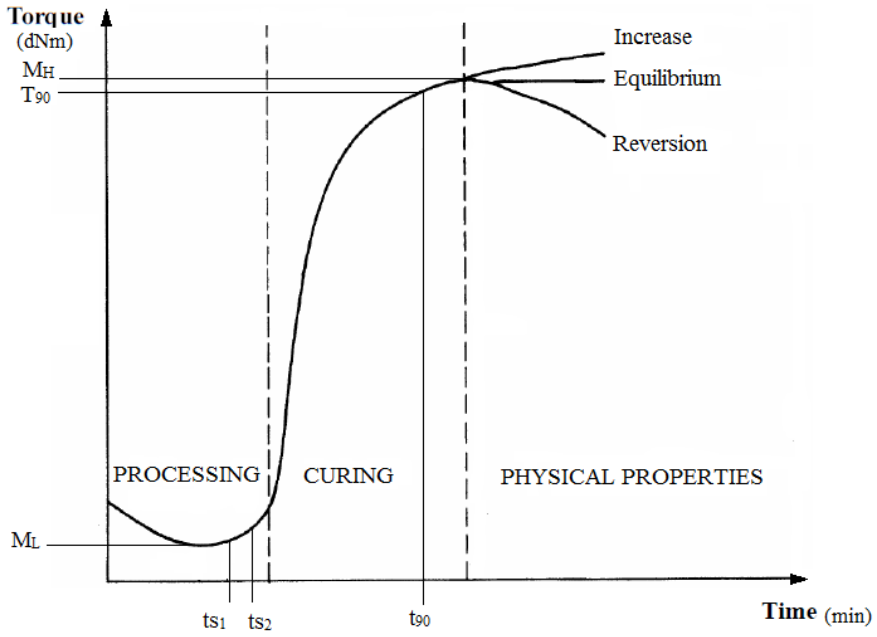

Figure 3.6: Typical schema of curing curve by rheometer [67].

The processing phase, at which viscous (plastic) behavior of the compound is dominating, shows rubber processability and therefore presents useful indications about the fluency in the moulds. Meaningful results are M_L, ts_1 and ts_2. M_L, minimum torque is obtained during specified period of curing time in a crosslinking isotherm for elastic response. M_L presents minimum viscosity value for compound. ts_1 or ts_2 refer to required time for the increase of 1 (ts_1) or 2 (ts_2) points from minimum torque. This number of time is called as "scorch time", and after this time, process of crosslinking starts. Scorch time is defined as indication of the time at which the first sign of crosslinking occurred. It is very important to know this value, especially during extrusion processes, because an unwanted scorch may cause dirtiness. As a result of this situation, will be needing of frequent cleanings of the extruder with loss of productivity. However, it depends on the applications because more scorch time will increase the processing time which will increase the production cost.

During the curing phase of the curve, the cross-linking process is evaluated. Typical data that can be obtained from the curve are t_{10}, t_{50}, and t_{90} which are the indications of the time at which achieve 10%, 50% and 90% curing, respectively. t_{90} refers to "optimum vulcanization time" [12].

The third and last part of the curve shows the physical properties of the rubber compound. The maximum value of torque (M_H) is the typical data of this part of

curve. M_H, maximum torque is presents maximum viscosity value for compound. This value is connected with the final level of crosslinking, the filler used, the compounding process and the quality of polymer used. After M_L value, degradation of compound can be measured. If any reversion occurs, it shows that rubber compound has resistance at high temperatures and it may be useful for the design of the transformation process.

3.2.2.4 Hot press

Hot press was used to carry out curing and molding (compression) processes of compound during optimum cure time at 192 °C under 150 bar pressure. A schema of basic two plates, single cavity hot press can be seen at Figure at 3.7.

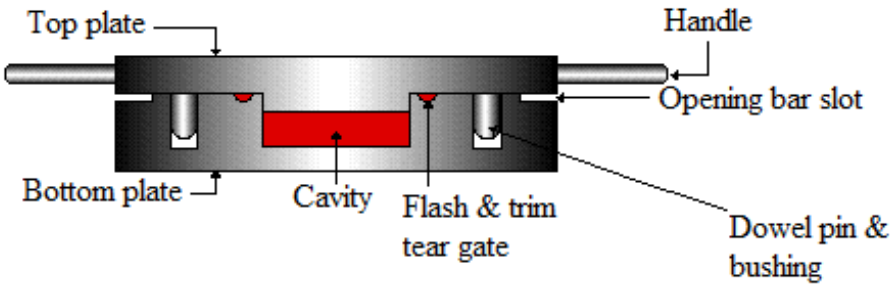

Figure 3.7: Schema of basic two plates, compression mold hot press [68].

Compression molding by hot press is the oldest and still most universally used technique in many aspects. This way is the cheapest process for many products because it is suitable for short periods and has low mold costs.

The hot press used for curing and molding has two platens which are heated either electrically or by saturated steam under pressure. The platens are brought together by pressure applied hydraulically either by water or oil, to give a loading of from 75 bar to 150 bar on the designed mold cavity area [13].

3.2.3 Equipments used for vulcanized compounds

3.2.3.1 Tensile test machine

Tensile properties of both EPDM rubber and EPDM/HNTs rubber were evaluated by Zwick Z010 universal tensile testing machine equipped with an extensometer. Load cell was 2 N and tensile properties of specimens were measured at 500 mm/min test speed. Gage length of sample was 20 mm. Universal tensile testing machine used according to ISO 37 type 2 is shown at Figure 3.8.

Figure 3.8: Universal tensile testing machine. (photo by Polat Yağmur, 2013.)

3.2.3.2 Shore durometer and international rubber hardness degrees tester (IRHD)

Before and after deformation tests (at -10 °C and 23 °C, 72 hours), hardness of rubber samples of 6 mm thickness was measured by Shore A type durometer. Durometer used according to ISO 7619-1 is shown at Figure 3.9. The effect of aging test (at 70 °C, 168 hours) on hardness of rubber samples (as tensile test specimens) was measured by IRHD (International rubber hardness degrees) micro compact hardness tester according to ISO 7619-1 is shown at Figure 3.10.

Figure 3.9: Shore A type durometer. (photo by Polat Yağmur, 2013.)

Figure 3.10: IRHD tester. (photo by Polat Yağmur, 2013.)

3.2.3.3 Deformation/compression set apparatus

Compression set of rubber components is defined as the difference between their original thickness and the thickness after compression and subsequent recovery. The permanent deformation remaining after release of a compressive stress was investigated by using compression set apparatus according to ISO 815. This compression set apparatus is shown in Figure 3.11. The thickness of original specimens were measured. Then, the specimens were placed between spacers and in the compression device. The specimens were compressed 25% of their original height for a specified time at a specified temperature (i.e. for 24 hours at 70 °C). After removing the sample from the oven, the specimens were allowed to cool for 30 minutes before measuring the final thickness.

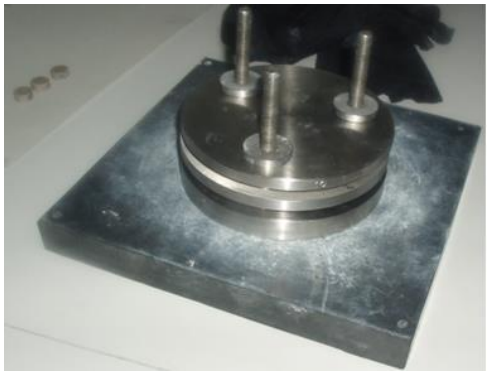

Figure 3.11: Compression set apparatus. (photo by Polat Yağmur, 2013.)

3.2.3.4 Heating oven

Heating oven (Binder GmbH) was used on the purpose of aging test (at 70 °C).

3.2.3.5 Thermogravimetric analyser (TGA)

Thermogravimetric analysis measures the amount and rate of weight changes in a material as a function of temperature or time in a controlled atmosphere [9]. Thermogravimetric analyser (Seiko Exstar 6200 TG/DTA) was used to make determinations about composition and thermal stability of EPDM rubber and EPDM/HNTs nanocomposites.

3.2.3.6 X-Ray diffractometer (XRD)

X-ray diffractometer (Panalytical X'Pert Powder) was employed for characterization and identification of polycrystalline phases in EPDM rubber and EPDM/HNTs nanocomposites.

X-ray diffraction (XRD) is a non-destructive analytical technique that X-ray reflection from crystalline materials is investigated to obtain a unique "X-ray fingerprint". X-ray fingerprint of a crystalline material is X-ray intensity versus scattering angle. Each material has own X-ray fingerprint associated with a crystal structure. X-Ray diffraction (XRD) patterns of the samples were recorded by monitoring the diffraction angles (2θ) from 2° to 20° on the diffractometer, using CuKα radiation. The wavelength used was $\lambda = 1.5405$ Å.

3.3 Methods

3.3.1 Preparation of compounds

In this work, two kinds of EPDMs (Keltan 778Z and Keltan 6950) were used for the nanocomposite samples productions. Each of EPDM types were used with different phr values of HNT and without HNT. Components of rubber samples and nanocomposites were mixed by laboratory type two-roll mill. EPDM, filler (HNTs), zinc oxide, stearic acid, activator (TAC), and peroxide (di(tert-butylperoxyisopropyl) benzene) were put to the two-roll mill, respectively. Labeling methods of compositions are shown at Figure 3.12. Composition recipes of HNTs filled and unfilled Keltan 778 and Keltan 6950 nanocomposites are shown at Table 3.1.

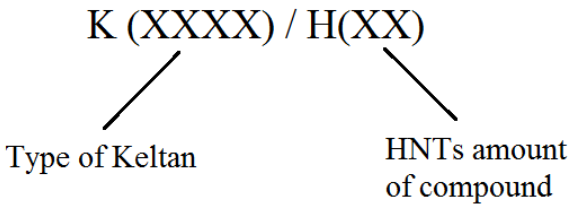

Figure 3.12: Labeling method of EPDM /HNTs nanocomposites.

Table 3.1: Compositions of HNT filled and unfilled Keltan 778Z and Keltan 6950 nanocomposites.

Composite (phr)	**K778Z/H0**	**K778Z/H10**	**K778Z/H20**	**K778Z/H40**	**K6950/H0**	**K6950/H10**	**K6950/H20**	**K6950/H40**
Keltan 778Z	100	100	100	100	-	-	-	-
Keltan 6950	-	-	-	-	100	100	100	100
HNT	-	10	20	40	-	10	20	40
ZnO	5	5	5	5	5	5	5	5
Stearic acid	1.5	1.5	1.5	1.5	1.5	1.5	1.5	1.5
TAC	2	2	2	2	2	2	2	2
Peroxide	7	7	7	7	7	7	7	7

3.3.2 Characterization of compounds

3.3.2.1 Curing characteristics

Curing properties (M_L and M_H) and curing times (ts_2, t_{90}) were evaluated with MDR at 192 °C. MDR was used according to ASTMD 5289. The Mooney viscosity M_L (1+4) was obtained as a value of torque in Mooney unit by MV at 100 °C. At the end of the preheating time (1 min), the initial peak viscosity (the initial maximum torque) was reached. After test running time (4 min) - therefore 5 min later since the test beginning- M_L (1+4) was determined. After stopping of rotor, the Mooney relaxation of rubber sample (i.e., the decrease of torque in time) was seen in the Mooney viscosity curve.

3.3.3 Preparation of EPDM nanocomposites

Hot press was used to carry out curing and molding (compression) processes of compound. The compounds were subsequently compression molded as sheet of 2

mm thickness at 192 °C, based on the respective t_{90} values. The curing times showed change according to type of EPDM and amount of HNT in nanocomposites. After curing, test samples were prepared in regard to required dimensions from cured sheets of 2 mm thickness.

3.3.4 Characterization of EPDM nanocomposites

3.3.4.1 Tensile test

Values of tensile properties of the cured samples (tensile strength, elongation at break, young modulus) were evaluated by use of universal testing machine equipped with an extensometer. Universal tensile testing machine used according to ISO 37-2. Tensile test was practiced at 500 mm/min test speed. At least, 3 samples were used for measurements. The error margins of tensile strength, elongation at break and young modulus calculated as ±0.1 MPa, 12% and 0 MPa, respectively. Test samples, which were prepared in regard to standardization, can be seen at Figure 3.13.

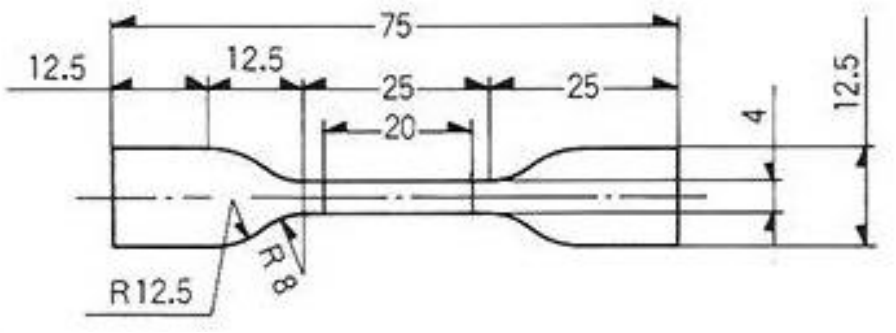

Figure 3.13: Tensile test sample for ISO 37-2 [69].

3.3.4.2 Hardness test

Hardness of initial and final states of rubber samples were compared during deformation and aging tests according to ISO 7619-1. Shore A type durometer and IRHD micro compact hardness tester were used for deformation and pre- & post-aging tests, respectively. Shore A type durometer was employed for deformation test samples of 6 mm thickness. On the other hand dumbbell shaped specimens were used for aging tests. Hardness test was carried out three times for one kind of nanocomposite sample and their average values were calculated.

3.3.4.3 Compression set A

Compression set of rubber samples of 6 mm thickness was investigated as the difference between their original thickness and the form after compression and subsequent recovery at 70 °C. Compression set test was obtained by using compression set apparatus according to ISO 815.

3.3.4.4 Crosslinking density (CLD)

Crosslinking density (CLD) of nanocomposites was evaluated by use of tensile modulus (M100) values which were calculated by stress-strain curves at constant temperature. Sekkar et al. worked on stress–strain curves to calculate CLD for the allophanate–urethane networks based on hydroxyl-terminated polybutadiene and toluene diisocyanate [9]. According to Sekkar et al. used Equation 3.1 for calculation of CLD, E is related to CLD.

$$E = 3\upsilon RT \quad \textbf{(3.1)}$$

where υ is CLD, R is universal gas constant (8.314 J $mol^{-1}K^{-1}$) and T is the constant temperature.

CLD calculation as evaluated from stress–strain curves is an advantageous and useful approach than swelling or similar procedures which need additional preparations.

3.3.4.5 Thermogravimetric analysis (TGA)

TGA analysis was performed using a TGA analyser from 25 °C to 800°C at a heating rate of 10 °C / min under nitrogen atmosphere.

3.3.4.6 X-ray diffraction analysis (XRD)

The XRD patterns of HNTs and EPDM/HNT nanocomposites with addition of 10 phr, 20 phr and 40 phr of HNT were recorded by a X-ray diffractometer. The basal spacing between layers of HNT was calculated by using Bragg's equation ($n\lambda = 2\,d\sin\theta$) taking n=1.

4. RESULTS AND DISCUSSION

In this study, HNTs were used as nanoclay fillers to improve mechanical and thermal properties of both Keltan 778Z and Keltan 6950 that had different ethylene/propylene ratios (crystallinity) and ENB contents. Test results were evaluated according to two parameters of nanocomposites: amount of HNTs in the nanocomposites and type of EPDMs. Compounds were prepared by using laboratory type two-roll mill. It was realized that whilst of HNTs contents, dispersibility of HNTs was decreasing in EPDM matrix. Due to this problem, maximum amount of HNTs was 40% of EPDM/HNTs compounds. Eight samples that included HNTs with from 0 to 40 phr values were prepared by using two types of EPDMs. Densities of EPDM/HNTs compounds were done to determine weight of samples that would be put into certain volume of basic two plates hot press to cure and mold. The density values of HNTs filled and unfilled Keltan 778Z and Keltan 6950 compounds were between 0.9 g/cm^3 and 1.05 g/cm^3 by using the instrument given in Section 3.2.2.1. Curing parameters and curing times of compounds were examined by using MDR. The curing parameters, curing times and Mooney viscosities of compounds were measured by using the techniques given in Section 3.3.2.1. The measurements results are also given and discussed in Section 4.1. Curing and molding processes of compounds were carried out by basic two plates hot press during determined time by MDR and optimum cure temperature at 192 °C. Mechanical properties of nanocomposites samples (i.e. tensile strength, elongation at break, tensile modulus) were examined by using universal tensile testing machine. HNTs contents and ethylene-propylene ratios of EPDMs had a remarkable effect on the tensile properties of HNT filled EPDM rubbers. Crosslinking densities (CLD) of nanocomposites were calculated by application of tensile modulus (M100) values to a special equation. Deformation ratios were examined by use of compression set apparatus. Rubber aging tests were performed for 168 hours at 70 °C. After aging test, tensile tests were practiced for aged nanocomposite samples to compare pre-aging and post-aging

states. In addition to this, hardness of pre- and post-aging states of nanocomposites were measured by using Shore A type durometer and international rubber hardness degrees tester (IRHD). The results about mechanical properties and CLD were given and discussed in Section 4.2.5. Thermal stabilities and compositions of nanocomposite samples were determined by using thermal gravimetric analyser (TGA). The explanations about TGA results were discussed in Section 4.3.1. Morphological properties were observed by using X-ray diffraction (XRD) analyser that provided observing of the basal spacing state of HNTs. XRD results with graphs were explained in Section 4.4.1.

4.1 Curing Properties of Compounds

There is no doubt to say that curing process creates irreversible alterations in rheology of rubber. It is well known, rheometer measurements provide a knowledge to decide availability and utility of using rubber in the sense of application area.

Scorch time (ts_2), optimum curing time (t_{90}) and the important curing parameters, M_L and M_H of EPDM/HNTs compounds are investigated by using MDR at 192 ^{0}C. The numerical values of curing times and curing parameters of each of EPDM/HNTs compounds are shown in Table 4.1.

Table 4.1: Rheological properties of EPDM/HNTs compounds.

	K778Z/H0	**K778Z/H10**	**K778Z/H20**	**K778Z/H40**	**K6950/H0**	**K6950/H10**	**K6950/H20**	**K6950/H40**
ts_2 (min)	0.29	0.37	0.35	0.31	0.29	0.32	0.30	0.29
t_{90} (min)	1.20	1.22	1.19	1.13	1.21	1.18	1.16	1.13
M_L (dNm)	1.42	1.70	1.89	2.28	2.45	2.60	2.85	3.20
M_H (dNm)	22.2	12.3	11.9	14.6	21.2	16.0	18.9	20.3

As can be seen in the Table 4.1, the ts_2 values of K778Z/H0 and K6950/H0 EPDM rubbers are shorter than nanocomposites with HNTs. These observations might be

due to EPDM penetrates into tubular structures of HNTs to form an interaction that makes delay in the onset of the composites. ts_2 values of EPDM/HNTs nanocomposites, which are the time for the onset of cure, decrease while HNTs loading of nanocomposites increase. These results about ts_2 indicate that with increasing the HNTs loading, the amount of active peroxide agents increase. Thus, more crosslinks are formed and shorter scorch times are recorded. It is also observed that after completion of penetration of EPDM into the tubular structures of HNTs, there is not any reason for delay of curing. So, t_{90} ,the cure time values of K778Z/H10, K778Z/H20, K778Z/H40 and K6950/H10, K6950/H20, K6950/H40 nanocomposites are shorter relative to unfilled K778Z/H0 and K6950/H0, respectively. Moreover t_{90} values decrease, by increasing of HNTs loading of nanocomposites.

The effects of HNTs loading on M_H of both HNTs filled Keltan 778Z and Keltan 6950 nanocomposites are shown in Figure 4.1.

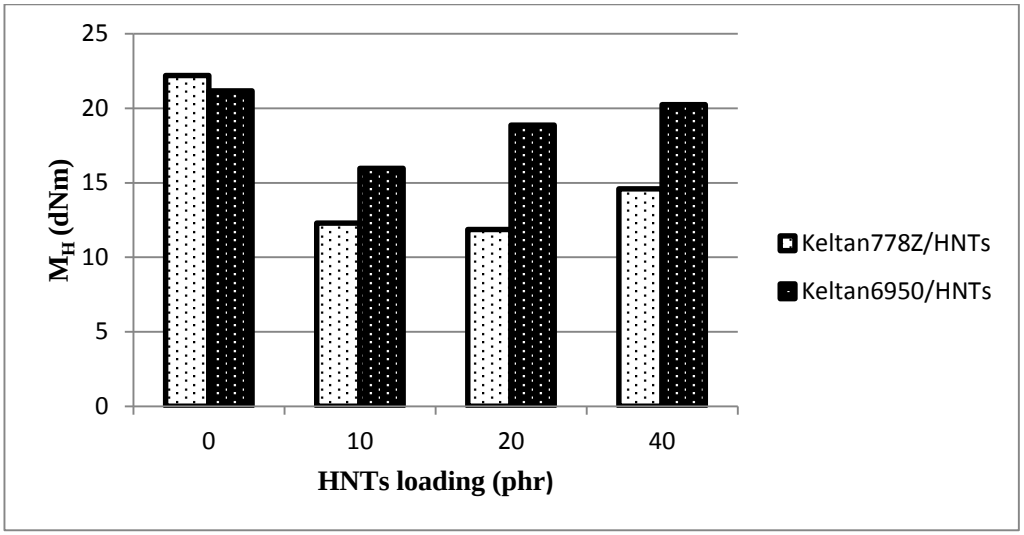

Figure 4.1: The effect of HNTs content on the M_H of EPDM/HNTs nanocomposites.

When the interfacial and intertubular adhesions between EPDM and HNTs increase, M_H increases [70]. The mobility of the macromolecular chains of the EPDM might decrease by the interaction between HNTs and EPDM as well as the intertubular reactions between the aluminols and silanols on the surfaces and edges of the HNTs, and consequently increase the stiffness of composites. As can be seen in Figure 4.1, M_H values of Keltan 6950/HNTs nanocomposites higher than Keltan 778Z/HNTs for the same HNTs and additive amounts. It proves that Keltan 6950/HNTs nanocomposites has better interactions between HNTs and EPDM. On the other

hand, when the M_H values of both K778Z/H0 and K6950/H0 are compared, K778Z/H0 has the higher one. Because for these nanocomposites, HNTs are not the matter of compounds. So, EPDM properties are dominant here that ethylene ratio of Keltan 778Z is more than Keltan 6950 one. Crystallinity is found to increase with the increase in ethylene content [71]. Although the crystallinity of Keltan 778Z is higher, consequently stiffness and M_H increases.

The cure rate indexes (CRI) of the EPDM/HNTs compounds are calculated according to Equation 4.1.

$$CRI = 100 / (t_{90} - ts_{2)} \quad \textbf{(4.1)}$$

Higher level of ENB (the diene monomer) brings about faster cure rate for sulphur vulcanizations. ENB ratios of Keltan 778Z and Keltan 6950 are 4.3% and 9%, respectively. According to these ENB ratios, cure rates of Keltan 6950 was expected higher than Keltan 778Z. As can be seen in Figure 4.2, the results are different than expectation. Because, despite using sulphurating agents, peroxide curing agents were used even though Keltan 778Z and Keltan 6950 have diene groups (termonomer). In this study peroxide curing was preferred, because of some advantages. In addition to improve performance and provide longer service life of EPDM rubbers, peroxide curing can also improve high temperature resistance, and reduce compression set [71]. There is no doubt to say that, the pronounced effect about the cure rates are the ethylene ratios for peroxide cured EPDM/HNTs compounds. Curing rates increase with the increasing of ethylene content [53]. As can be seen in Figure 4.2, this result proves that ethylene content of Keltan 778Z is higher than Keltan 6950.

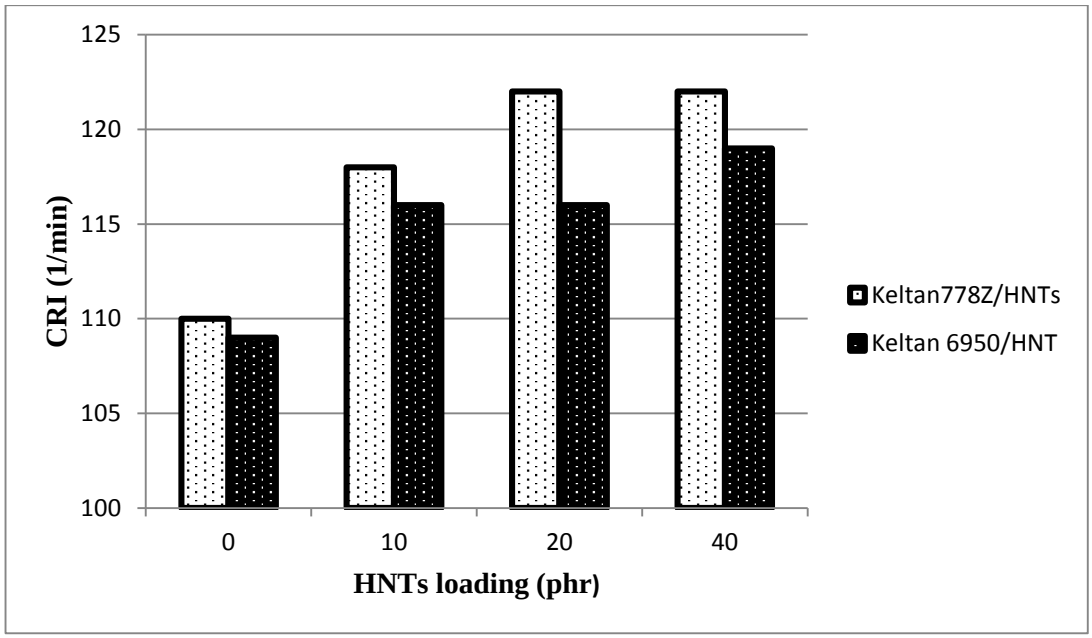

Figure 4.2: The effect of HNTs loading and ENB contents on cure rates.

Mooney viscosities (M_L (1+4)) of Keltan 778Z/HNTs and Keltan 6950/HNTs compounds were examined by MV at 100 °C. Viscosity of a rubber presents mechanical processing ability. The most commonly used method to evaluate viscosity of rubbers is Mooney viscosity determination. The numerical values of M_L (1+4) can be seen in Table 4.2.

Table 4.2: Mooney viscosity values of EPDM/HNTs compounds.

	K778Z/H0	**K778Z/H10**	**K778Z/H20**	**K778/H40**	**K6950/H0**	**K6950/H10**	**K6950/20**	**K6950/40**
M_L (1+4) (MU)	73.8	86.0	91.5	103.6	116.3	113.6	117.7	129.1

As can be seen in Table 4.2, Mooney viscosity shows an increase while HNTs content is increasing for Keltan 778Z/HNTs compounds. In addition, the same increasing behavior can be seen also for Keltan 6950/HNTs compounds, except K6950/H10. This exception might be neglect because of the numerical difference is not extreme.

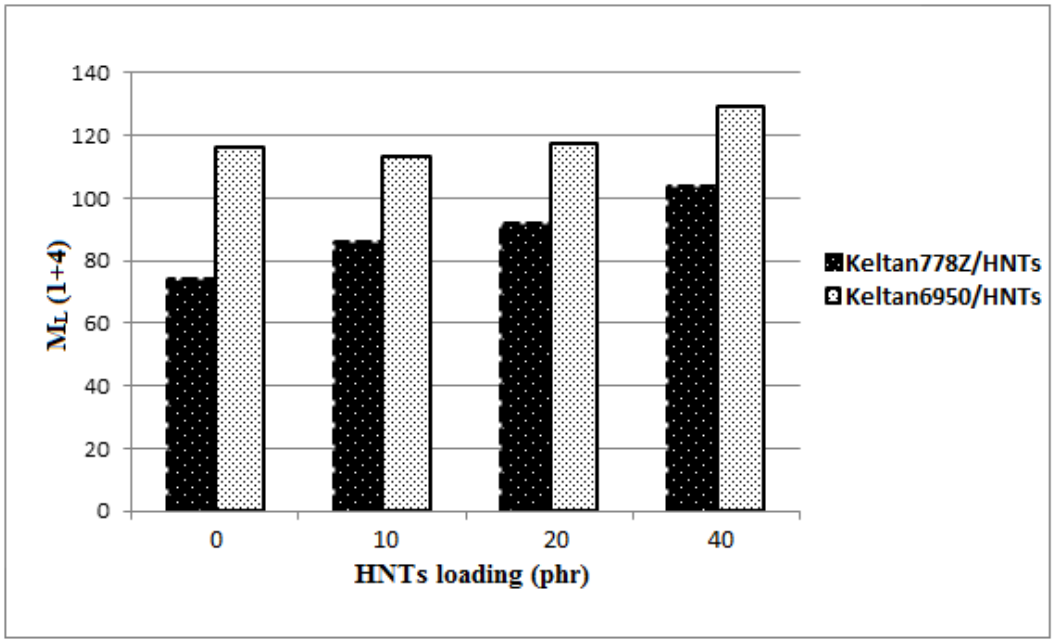

Figure 4.3: The effect of HNTs loading on different ethylene/propylene ratios.

Figure 4.3 shows the effect of HNTs loading on the ethylene/propylene ratios of EPDM rubbes types. Keltan 6950/HNTs compounds have higher M_L (1+4) values than Keltan 778Z. This result indicates that processability of Keltan 6950/HNTs nanocomposites is also higher than Keltan 778Z/HNTs nanocomposites. It is well known that halloysite makes rubbers easy-processable. In addition, according to M_H values, it is understood that Keltan 6950/HNTs nanocomposites has better interactions between HNTs and EPDM. So the test results of MDR are in agreement with MV.

4.2 Mechanical Properties of EPDM/HNTs Nanocomposites

4.2.1 Tensile tests of nanocomposites

Tensile properties of both Keltan 778Z/HNTs and Keltan 6950/HNTs rubbers were evaluated by universal tensile testing machine that used according to ISO 37 type and the error margins calculated as as mentioned in Section 3.3.4.1. Tensile modulus, tensile strength and elongation at break of the EPDM/HNTs nanocomposite samples can be directly obtained from the recorded stress–strain curves. Tensile modulus (M100), tensile strength (σ) and elongation at break (ε) values are shown in Table 4.3.

Table 4.3: Tensile properties of EPDM/HNTs nanocomposite samples.

	Tensile modulus (MPa)	Tensile strength (MPa)	Elongation at break (%)
K778Z/H0	1.7	2.9	189
K778Z/H10	1.5	5.2	504
K778Z/H20	1.7	5.1	535
K778Z/H40	1.9	5	512
K6950/H0	1.7	2.1	133
K6950/H10	1.3	2.4	289
K6950/H20	1.5	2.4	250
K6950/H40	1.7	2.5	226

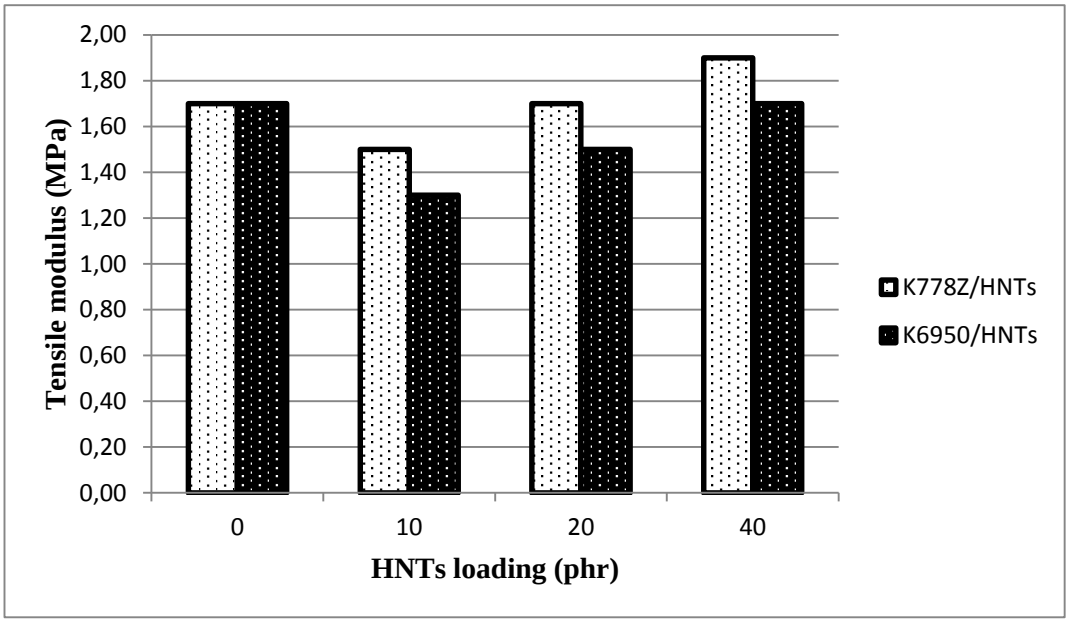

Figure 4.4: The effect of HNTs loading on tensile modulus values of both Keltan 778Z/HNTs and Keltan 6950/HNTs nanocomposites.

M100 values are used to describe elastic properties of nanocomposite samples. Figure 4.4 shows the effects of HNTs loading on different kind of EPDM rubbers (Keltan 778Z and Keltan 6950). When a comparison of M100 values of Keltan 778Z/HNTs nanocomposites is made in itself, it is seen that there is a significantly increase whilst HNTs loading increase. For instance, M100 value of the K778Z/H40 is 27% higher than K778Z/H10. The increasing of M100 values of Keltan 6950 is also provided by increasing of HNTs loading. For example, the M100 values of

K6950/H40 is 31% higher than Keltan 6950/H10. Increasing percentages of M100 values of HNTs filled Keltan 6950 nanocomposites is more than HNTs filled Keltan 778Z nanocomposites. Ismail et al. reported that the increasing of the M100 values of EPDM/HNTs nanocomposites by increasing of HNTs loading is related to the good interactions between HNTs and EPDM matrix [52]. From this point of view, Keltan 6950 has better interactions with HNTs than Keltan 778Z. There is no doubt to say that M100 results are in conformance with MV and MDR measurements. However, there is an exceptional situation for each of EPDM types that unfilled EPDM rubbers have higher M100 values than filled EPDM nanocomposites with 10% HNTs. But, this situaiton can be ignored because of the continuous increasing values of modulus values whilst HNTs loading increase.

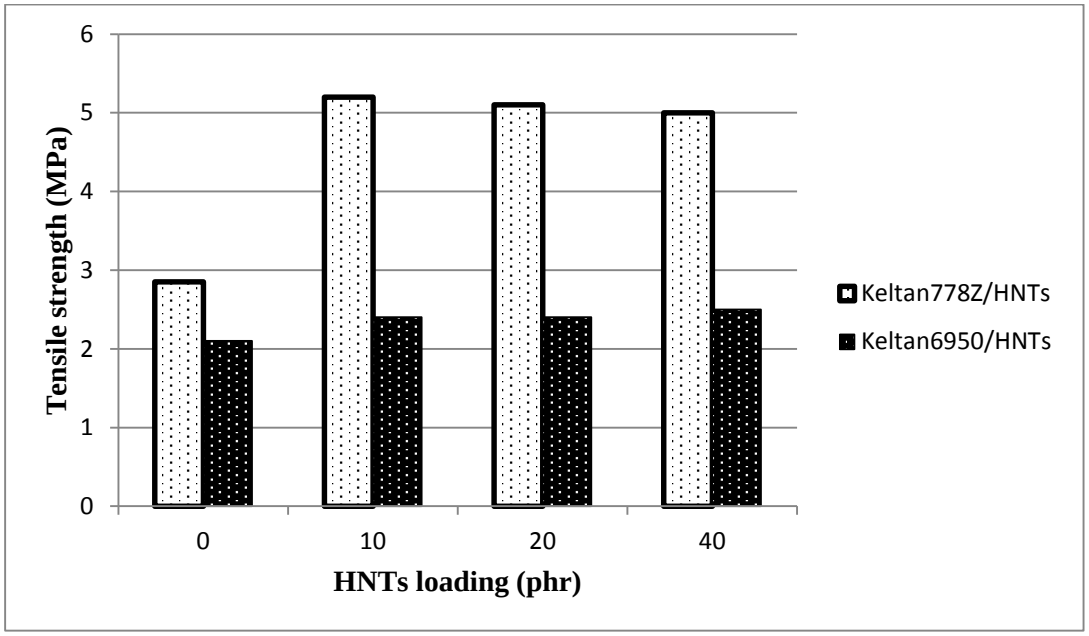

Figure 4.5: The effect of HNTs loading on tensile strength values of both Keltan 778Z/HNTs and Keltan 6950/HNTs nanocomposites.

Figure 4.5 illustrates the enhancement in tensile stress while increasing amount of HNTs in Keltan 778Z/HNTs and Keltan 6950/HNTs nanocomposites. As can be seen in Figure 4.5, tensile strength values of Keltan 778Z/HNTs nanocomposites are higher than Keltan 6950/HNTs nanocomposites one. It is mentioned in Section 2.3.2.2 that high-ethylene EPDM grades have higher tensile strength. As a result, it is clear that ethylene content of Keltan 778Z is higher than Keltan 6950 one. The maximum tensile strength value of Keltan 778Z/HNTs is belongs to K778Z/H10, and it is 82% higher than unfilled K778Z/H0. The tensile strength slightly decreases

when HNTs contents are more than 10%. The maximum tensile strength value of Keltan 6950 is observed in K6950/H40 that is 19% higher than unfilled K6950/H0. The enhancement in tensile strength of filled EPDM nanocomposites is based on the dispersibility of HNTs in EPDM matrix and inter-tubular interactions between HNTs and EPDM [53]. Yang et al. reported that strong interactions provide more efficient load transfer and, hence, better mechanical performance [72].

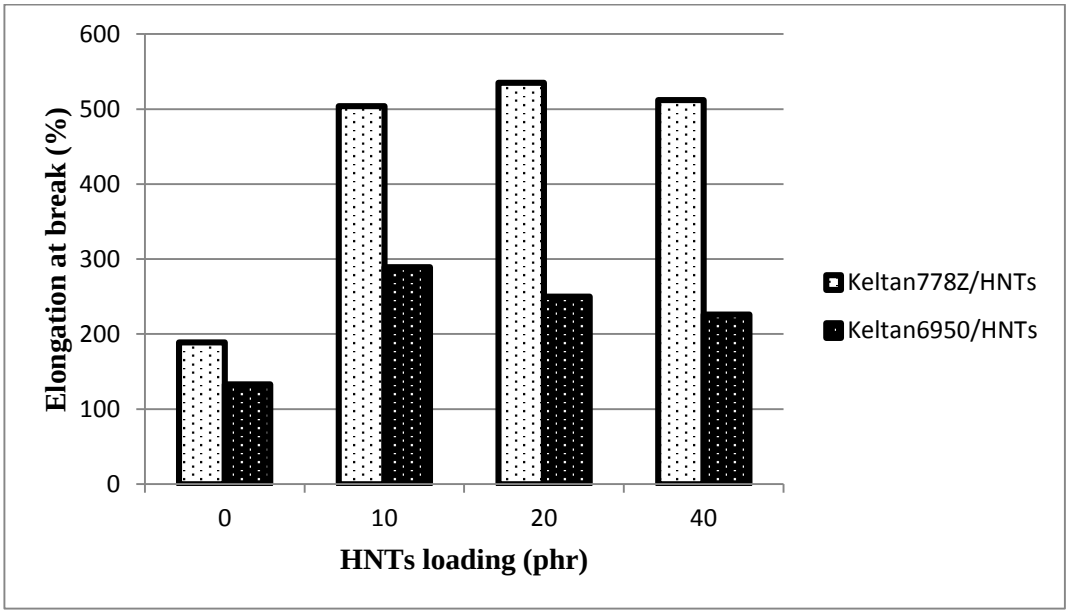

Figure 4.6: The effect of HNTs loading on ε values of both Keltan 778Z/HNTs and Keltan 6950/HNTs nanocomposites.

The effect of HNTs loading on ε values at break of both Keltan 778Z/HNTs and Keltan 6950/HNTs nanocomposites is shown in Figure 4.6. As can be seen, the ε values at break increase when HNTs is added to matrix. K778Z/H20 has the maximum value for ε at break in Keltan 778Z nanocomposites, K6950/H10 has the maximum value for ε at break in Keltan 6950 nanocomposites. Up to certain amount of HNTs ε increase for each of EPDM/HNTs nanocomposites. The ε value at break of the K778Z/H20 is 183% higher than unfilled K778Z/H0. In addition, the ε value at break of K6950/H10 is 117% higher than unfilled K6950/H0. Such simultaneous increases in tensile strength, stiffness (M100) and ductility (ε) of rubber composites is interesting and an advantage, which has been obtained by incorporation of HNTs in the EPDM.

4.2.2 Crosslinking densities of EPDM/HNTs nanocomposites

Crosslinking density (CLD) of nanocomposites was evaluated by use of tensile modulus (M100) values which were calculated by stress-strain curves at 23 °C. CLD values of both Keltan 778Z/HNTs and Keltan 6950/HNTs nanocomposites calculated as following Equation 3.1. The effect HNTs loading on CLD values of Keltan 778Z/HNTs and Keltan 6950/HNTs nanocomposites can be seen in Figure 4.7.

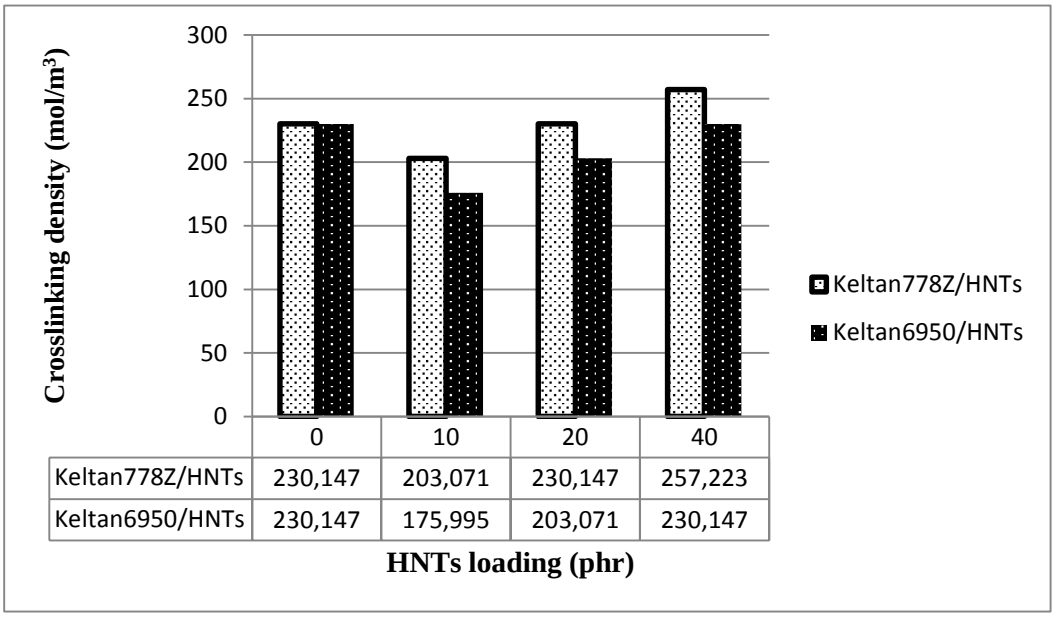

	0	10	20	40
Keltan778Z/HNTs	230,147	203,071	230,147	257,223
Keltan6950/HNTs	230,147	175,995	203,071	230,147

Figure 4.7: The effect of HNTs loading on CLD values of Keltan 778Z/HNTs and Keltan 6950/HNTs nanocomposites.

The crosslink density results are similar to tensile modulus graphs. For instance, K778Z/H0 and K6950/H0 have the higher CLD values than K778Z/H10 and K6950/H10, respectively. Moreover, CLD values of K778Z/H0 and K6950/H0 equal to K778Z/H20 and K6950/40, respectively. Nevertheless, the more importantly point is that there is a continuously increasing while HNTs loading increase. Therefore, there is no doubt to say that CLD values of the EPDM/HNTs nanocomposites increase with addition of HNTs. CLD of K778Z/H40 is 27% higher than CLD of K778Z/H10. Also, CLD of K6950/H40 is 31% higher than CLD of K6950/H10. The increase in crosslinking is related to decrease in molecular weight. Stelescu et. al. reported that while the CLD increase, the chain mobility of macromolecules decrease, and therefore the rubber becomes stiffer [73]. Accordingly, while HNTs loading increase, molecular weight and stifness of both of Keltan 788Z/HNTs and Keltan 6950/HNTs decrease and increase, respectively. For matrix comparison, as

mentioned before and due to Figure 4.7, Keltan 778Z/HNTs nanocomposites are stiffer than Keltan 6950/HNTs nanocomposites. For instance CLD of K778Z/H20 is 13% higher than same amount HNTs filled K6950/H20.

4.2.3 Hardness tests of EPDM/HNTs nanocomposites

Hardness of EPDM/HNTs nanocomposites were compared during addition of HNTs into the EPDM matrix. Shore A type durometer was employed for both of the Keltan 778Z/HNTs and Keltan 6950/HNTs nanocomposite test samples of 6 mm thickness. Hardness test results can be seen in Table 4.4

Table 4.4: Hardness test results of EPDM/HNTs nanocomposites.

	K778Z/H0	**K778Z/H10**	**K778Z/H20**	**K778Z/H40**	**K6950/H0**	**K6950/H10**	**K6950/H20**	**K6950/H40**
Hardness (Shore A)	60	63	65	69	61	57	61	65

As can be seen in Table 4.4, hardness of Keltan 778Z/HNTs nanocomposites increase whilst HNTs contents increase in nanocomposites. For Keltan 6950/HNTs nanocomposites, there is no certain increase or decrease in hardness. The hardness test results show that hardness of Keltan 778Z/HNTs nanocomposites is better than Keltan 6950/HNTs. The most important factor of this situation is the difference of ethylene contents of Keltan 778Z and Keltan 6950 rubbers.

4.2.4 Deformation tests / compression set

Compression sets were measured to investigate ability of both Keltan 778Z/HNTs and Keltan 6950 nanocomposite samples to retain their elastic properties after prolonged compression for 24 hours at 70 °C and their permanent deformation. Table 4.5 illustrates the compression test results of both Keltan 778Z/HNTs and Keltan 6950 nanocomposites.

Table 4.5: Compression set values of EPDM/HNTs nanocomposites.

	K778Z/H0	K778Z/H10	K778Z/H20	K778Z/H40	K6950/H0	K6950/H10	K6950/H20	K6950/H40
Compression set (%) (24 hours, 70 °C)	5.6	12.7	19.1	18.3	4.3	4.7	4.1	6.4

As a rubber material is compressed for a certain time, it loses its ability to return to its original thickness. This loss of resiliency may reduce the capability of the rubber material to perform over a long period. Compressions set results for the rubber material are expressed as percentage of difference of initial thickness and final thickness. If the percentage is low, the material has the better resistance to permanent deformation. As can be seen in Table 4.5, apart from some exceptional situations, addition of HNTs to Keltan 778Z and Keltan 6950 causes higher compression sets than unfilled EPDM nanocomposites. The weakness of interactions of EPDM matrix and HNTs might be result in higher compression sets than unfilled EPDM nanocomposites.

4.2.5 Aging tests of EPDM/HNTs nanocomposites

Aging tests of Keltan 778Z/HNTs and Keltan 6950/HNTs nanocomposites were practiced under determined conditions (168 hours, 70 °C) by using heating oven. Aged nanocomposite samples were subjected to tensile tests and hardness test to find out the changes in tensile strengths, elongations at break and hardness values. Table 4.6 shows these changes in mentioned measurements after aging tests.

After aging tests, hardness changes are not remarkable for both Keltan 778Z/HNTs and Keltan 6950/HNTs nanocomposites for every amount of HNTs. Tensile strength value of unfilled K778Z/H0 does not show any change compared to before aging process. However, while tensile strengths of K778Z/10 and K778Z/20 decrease, tensile strength of K778Z/H40 increase. Tensile strength of unfilled K6950/H0 shows decrement. Nevertheless, tensile strength of K6950/H10 has the same value after aging test. K6950/H20 and K6950/H40 have increments in their tensile strength values. Due to these results, it is possible to say that there is no consistent situation after aging test about tensile strength changes.

After aging test, elongations at break of K778Z/H10, K778Z/H20, K778Z/H40 decrease and lose their ductilities, due to before. K778Z/H0 has higher value than pre-aging test. K6950/H0, K6950/H10, K6950/H20 and K6950/H40 decrease and they lose their ductilities compared to before as a result of aging tests. In brief, after aging tests, according to Table 4.6 results, test results are not suitable to make any commentary. Because after aging process, for all the test results of hardness, tensile strength and elongation at break, there are no any relative data.

Table 4.6: The changes in mechanical properties after aging test of EPDM/HNTs nanocomposites.

	K778Z/H0	**K778Z/H10**	**K778Z/H20**	**K778Z/H40**	**K6950/H0**	**K6950/H10**	**K6950/H20**	**K6950/H40**
Hardness change (Shore A)	0	+2	0	-1	+1	+1	0	+1
Tensile strength change (MPa %)	0	-9.6	-13.7	+4	-14.3	0	+12.5	+12
Elongation at break change (%)	+1.6	-7.5	-11.4	-5.3	-18.8	-10.4	-2	-7.5

4.3 Thermal Properties of EPDM/HNTs Nanocomposites

4.3.1 Thermogravimetric analysis (TGA) of EPDM/HNTs nanocomposites

Thermogravimetric analysis (TGA) of EPDM/HNTs nanocomposites were performed by using thermogravimetric analyser from 25 °C to 800°C at a heating rate of 10 °C / min under nitrogen atmosphere. The percentages of weight changes in EPDM/HNTs nanocomposites as a function of temperature were measured in a controlled atmosphere by TGA. Table 4.7 illustrates the TGA results of both Keltan 778Z/HNTs and Keltan 6950/HNTs nanocomposites.

As can be seen in Table 4.7, thermal stabilities of K778Z/H10 and K778Z/H20 are better than unfilled K778Z/H0 and K778Z/H40. According to these results the optimum amounts of HNTs for thermal stability in Keltan 778Z/HNTs nanocomposites are between 10-20 phr. Optimum value of HNTs for thermal stability of Keltan 6950/HNTs nanocomposites is 20 phr. Apart these optimum

values of HNTs, decomposition of both Keltan 778Z/HNTs and Keltan 6950/HNTs nanocomposites start in lower temperatures.

Table 4.7: TGA results of both Keltan 778Z/HNTs and Keltan 6950/HNTs nanocomposites.

	K778Z/H0	**K778Z/H10**	**K778Z/H20**	**K778Z/H40**	**K6950/H0**	**K6950/H10**	**K6950/H20**	**K6950/H40**
Temperature at onset decomposition (°C)	418	421	421	408	416	411	418	392
Temperature at 50% weight loss (°C)	473	475	476	470	469	470	472	465
Weight of residue after decomposition (%)	9	11	17	24	6	12	18	24

According to Table 4.7, these results are in agreement with temperatures at 50% weight loss of nanocomposites. Weight of residues of each EPDM nanocomposites after decomposition show increment, while HNTs amount increase. Increment of weight of residue of both Keltan 778Z/HNTs and Keltan 6950/HNTs are proportional with additional amount of HNTs. Thus, the major amount of residue might be belong to HNTs that include 43.3% SiO_2 and 38.4% Al_2O_3. Therefore, increasing of weight of residue after decomposition might prove the hardness of dispersibility of higher HNTs amount in EPDM matrix.

4.4 Morphological Properties of EPDM/HNTs Nanocomposites

4.4.1 X-Ray diffractometer analysis of EPDM/HNTs nanocomposites

Because of chemical formula, HNTs include interlayer water. The interlayer water in HNTs can be easily removed by heating. As a result of removing the interlayer water, the basal space between the layers of tubular structure is 7 Å, so it is 7 nm. The XRD patterns of HNTs and EPDM/HNTs nanocomposites with 0 phr to 40 phr of HNTs were recorded by a X-ray diffractometer. XRD pattern comparisons of HNTs in Keltan 778Z/HNTs and Keltan 6950/HNTs nanocomposites are shown in

Figure 4.8 and Figure 4.9, respectively. Figure 4.8 and Figure 4.9 illustrate HNTs peaks after addition of HNTs into EPDM matrix. Basal spaces of diffracting planes of HNTs are calculated for Keltan 778Z/HNTs and Keltan 6950/HNTs nanocomposites that can be seen in Table 4.8.

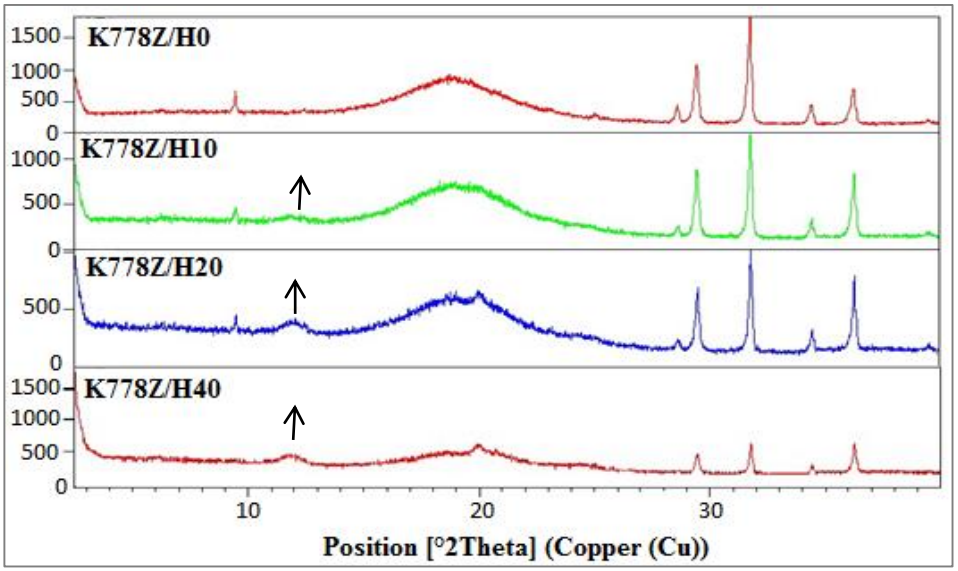

Figure 4.8: XRD patterns of Keltan 778Z/HNTs nanocomposites.

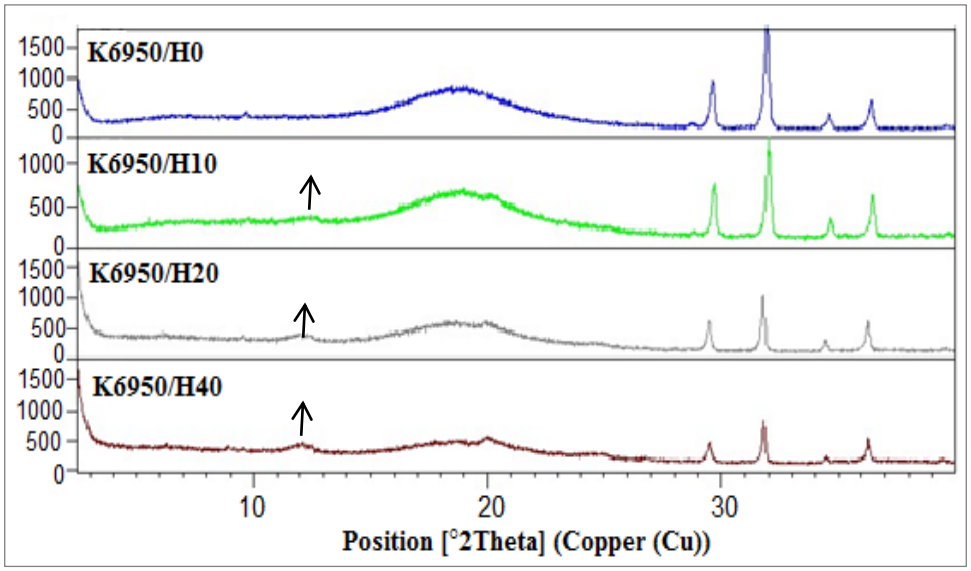

Figure 4.9: XRD patterns of Keltan 6950/HNTs nanocomposites.

The basal spaces of the layers in the samples were calculated from Bragg's equation (Section 3.3.4.6). The measured and calculated diffracting planes of HNTs increase, while HNTs amount increase both in Keltan 778Z/HNTs and Keltan 6950/HNTs nanocomposites. It is concluded that, due to these results, intercalation situation increase in high amounts of HNTs. However, these results also provide that basal

space measurements of Keltan 6950/HNTs are larger than Keltan 778Z/HNTs one. Better interaction between HNTs and Keltan 6950 than Keltan 778Z prove this situation. While interfacial adhesions increase between EPDM and halloysite, halloysite's dimensions enlarge. Therefore, XRD results are in conformance with M_H results.

Table 4.8: Basal spaces of diffracting planes of HNTs in Keltan 778Z/HNTs and Keltan 6950/HNTs nanocomposites.

	K778Z/H0	**K778Z/H10**	**K778Z/H20**	**K778Z/H40**	**K6950/H0**	**K6950/H10**	**K6950/H20**	**K6950/H40**
d (nm)	-	0.67	0.69	0.71	-	0.71	0.71	0.73

5. CONCLUSION

In this study, HNTs were used as reinforcement filler for different ethylene contents and ENB contents having EPDMs that were Keltan 778Z and Keltan 6950. Examinations revealed that HNTs dispersibility decreased after 40 phr HNTs amount. As a result of that, HNTs amount were taken into accounts for 0 phr, 10 phr, 20 phr and 40 phr. The curing times, curing parameters and Mooney viscosity values of EPDM/HNTs compounds were investigated by using MDR and MV, respectively. Mechanical properties of nanocomposite samples were measured by using universal tensile testing machine, Shore A type durometer and compression set apparatus. Thermal stability of nanocomposite samples were examined with TGA and morphological properties of HNTs were researched with XRD. The results of those experiments are summarized in this section.

EPDM penetration into lumen structure of HNTs delays scorchs of both K778Z/H10 and K6950/H10 nanocomposites, due to unfilled EPDM nanocomposites. Peroxide activator role of HNTs reduces the scorch times of both K778Z/H10 and K6950/H10 nanocomposites as mentioned in Section 4.1. The next observation about curing times is that optimum cure times of HNTs filled Keltan 778Z and Keltan 6950 nanocomposites are shorter relative to unfilled versions of them. Because, after completion of EPDM penetration into HNTs, there is no reason for delay of curing. In addition, investigations reveal that the optimum cure time decreases, by increasing the load of HNTs of Keltan 778Z/HNTs nanocomposites. M_H values of HNTs filled Keltan 6950 nanocomposites are measured as higher than HNTs filled Keltan 778Z nanocomposites for the same HNTs and additive amounts. From that point, it is concluded that HNTs filled with Keltan 6950 nanocomposites has better adhesions between HNTs and EPDM. However, the result of M_H of K778Z/H0 is higher than K6950/H0. Because for unfilled EPDM composites, the effective factor is ethylene ratio that is higher in Keltan 778Z. In brief, higher ethylene ratio brings about higher crystallinity, consequently more stiffness and higher M_H. CRI of Keltan 778Z/HNTs

nanocomposites are calculated higher than Keltan 6950/HNTs nanocomposites in the same amount of HNTs and other additives. Results of CRI prove that ethylene ratio is a important factor for curing rates. According to MV results, M_L (1+4) values of Keltan 778Z/HNTs nanocomposites increase while HNTs amount is increasing in polymer matrix. The same behavior is also observed for Keltan 6950/HNTs nanocomposites, except K6950/H10. However, due to lack of significant difference, this decrement is ignored. For comparison of polymer matrixes, it is examined that Keltan 6950/HNTs compounds have higher M_L (1+4) values than Keltan 778Z/HNTs compounds. Hence, it can be said that processability of Keltan 6950/HNTs nanocomposites is better than Keltan 778Z/HNTs nanocomposites one. Addition of HNTs to Keltan 778Z and Keltan 6950 provides increment of M100 values. As interactions between Keltan 6950 and HNTs are stronger, HNTs filled Keltan 6950 nanocomposites have more increasing percentages than HNTs filled Keltan 778Z nanocomposites. However, M100 values of K778Z/H0 and K6950/H0 are more than K778Z/H10 and K6950/H10, respectively. But for this study, the important point is the constantly increasing values of modulus values whilst HNTs' increase loads. HNTs enhance the tensile strength values of both Keltan 778Z/HNTs and Keltan 6950/HNTs in optimum amounts of its. These amounts are 10 phr and 40 phr for Keltan 778Z/HNTs nanocomposites and Keltan 6950/HNTs nanocomposites, respectively. On the other hand, tensile strength values of Keltan 778Z/HNTs nanocomposites are measured to be higher than Keltan 6950/HNTs nanocomposites. The explanation about this result might be that ethylene content of Keltan 778Z is higher than Keltan 6950 one. Elongation at break values of Keltan 778Z/HNTs and Keltan 6950/HNTs increase, while HNTs add into matrixes. The maximum elongation at breaks values are investigated K778Z/H20 and K6950/H10 for Keltan 788Z/HNTs and Keltan 6950/HNTs nanocomposites, respectively. These kind of simultaneous increases in tensile strength, M100 and elongation at break values (ductiliy) are advantage and interesting. Hardness values of Keltan 778Z/HNTs nanocomposites increase properly. However hardness values of Keltan 6950/HNTs nanocomposites do not show certain increment or decrement. Shore A type durometer measurements show that hardness values of Keltan 778Z/HNTs nanocomposites are stronger than Keltan 6950/HNTs nanocomposites, because of ethylene ratio effect. Apart from the some exceptional situations, addition of HNTs to Keltan 778Z and Keltan 6950 causes higher compression sets than unfilled EPDM

nanocomposites. In addition, compression set values of Keltan 778Z/HNTs nanocomposites are more than Keltan 6950/HNTs. This result is about interactions between EPDM and HNTs and in agreement with MDR results. CLD values of the EPDM/HNTs nanocomposites show increment with addition of HNTs. The increase of CLD is related to decrement of molecular weight. For better thermal stability, TGA tests result that optimum HNTs amount for Keltan 778Z/HNTs and Keltan 6950/HNTs nanocomposites are between 10-20 phr and 20 phr, respectively. Investigation of morphological properties of HNTs by XRD show that the basal space of HNTs increase, while HNTs amount increase in nanocomposites. It is understood that, due to these results, intercalation situation increases in high amounts of HNTs.

In conclusion, HNTs provide simultaneous increases in tensile strength, M100 and elongation at break values (ductiliy) of Keltan/HNTs nanocomposites, that is advantageous and interesting result for rubber studies.

REFERENCES

[1] **Nabil, H., Ismail, H., Azura, A. R.** (2013). Compounding, mechanical and morphological properties of carbon-black-filled natural rubber/recycled ethylene-propylene-diene-monomer (NR/R-EPDM) blends. *Polymer Testing*, ***32,*** No:2, 385-393.

[2] **Simpson, R.B.** (2002). Rubbers in *Rubber Basics (1st ed.),* 75-116, Rapra Technology Ltd., Shropshire, United Kingdom.

[3] **Salamone, J. C.** (1996). Ethylene-Propylene Elastomers in *Polymeric Materials Encyclopedia (Vol. 3),* 2264-2271, CRC Press, The United States of America.

[4] **Martinez L., Nevshupa R., Felhos D., De Segovia J.L., Roman E.** (2011). Influence of friction on the surface characteristics of EPDM elastomers with different carbon black contents. *Tribology International*, ***44,*** 996-1003.

[5] **Koo, J. H., Pilato, L. A., Wissler G. E.** (2007). Polymer Nanostructured Materials for Propulsion Systems. *Journal of Spacecraft and Rockets*, ***44,*** No:6, 1250-1262.

[6] **Kamble, R., Ghag, M., Gaikawad, S., Panda, B. K.** (2012). Halloysite Nanotubes and Applications: A Review. *Journal of Advanced Scientific Research*, ***3,*** No:2, 25-29.

[7] **Rawtani, D., Agrawal, Y. K.** (2012). Multifarious Applications of Halloysite Nanotubes: A Review. *Material Science*, ***30,*** 282-295.

[8] **Onokpise, O. U.** (2003). Rubber in *Magill's Encyclopedia of Science:Plant Life (1st ed.) (Vol. 3),* 925-929, Ness, B. D. (Ed.), Salem Press, California, The United States of America.

[9] **De, S. K., White, J. R.** (2001). *Rubber Technologist's Handbook*, Rapra Technology Ltd., Exeter, United Kingdom.

[10] **Raue, M., Wambach, M., Glöggler, S., Grefen, D., Kaufmann, R., Abetz, C.** (2014). Investigation of Historical Hard Rubber Ornaments of Charles Goodyear. *Macromolecular Chemistry and Physics*, ***215***, 245-254.

[11] **Hertz, D. L.** (2001). Introduction in *Engineering with Rubber:How to Design Rubber Components, (2nd ed.),* Gent, A. N. (Ed.), Hanser Publishers, Munich, Germany.

[12] **Chandrasekaran, V.C.** (2010). *Rubber as a Construction Material for Corrosion Protection*, Scrivener Publishing, The United States of America.

[13] **Ma, J., Zhang, L-Q, Geng, L.** (2010). Manufacturing Techniques of Rubber Nanocomposites in *Rubber Nanocomposites: Preparation, Properties and Applications*, 21-61, Thomas, S., Stephen, R. (Eds.), John Wiley&Sons Pte Ltd, Singapore.

[14] **Url-1** <*http://chemed.chem.purdue.edu/genchem/topicreview/bp/1polymer/terms.html*>, date retrieved 24.02.2014.

[15] **Url-2** <*http://www.chemistrylearning.com/rubber/*>, date retrieved 25.02.2014.

[16] **Puskas J. E., Chiang, K.** (2014). Natural Rubber Biosynthesis: Perspsctives from Polymer Chemistry, in *Chemistry, Manufacture and Applications of Natural Rubber*, 30–67, Kohjiya, S., Ikeda, Y. (Eds.), Woodhead Publishing, Cambridge, United Kingdom.

[17] **Vijayaram, T. R.** (2009). A Technical Review on Rubber, *International Journal on Design and Manufacturing Technologies, **3***, No:1, 25-37.

[18] **Li, M., Li, Y., Zhang, J., Feng, S.** (2014). Effect of Compatibilizers on the Miscibility of Natural Rubber/Silicone Rubber Blends. *Polymer Engineering & Science, **54,*** No:2, 355-363.

[19] **Rodgers, B., Waddell W.** (2005). The Science of Rubber Compounding in *Science and Technology of Rubber (3rd)* , 401-454, Mark, J.E., Erman, B., Eirich, F. R. (Eds.), Elsevier Academic Press, London, United Kingdom.

[20] **Url-3** <*http://www.tis-gdv.de/tis_e/ware/kautschuk/synthesekautschuk/synthesekautschuk.htm)*>, date retrieved 10.03.2014.

[21] **Malaysian Rubber Board** (2013). World Rubber Consumption in *Natural Rubber Statistics.*

[22] **Furlan, L. G.** (2005). Early and Post Transition Metal Complexes as a Single or Combined Components in the Ethylene and Isoprene Polymerization, Ph. D. Thesis, University of Federal do Rio Grande do Sul.

[23] **Ebewele, R. O.** (2000). Polymer Properties and Applications in *Polymer Science and Technology*, 413-471, CRC Press, Florida, The United States of America.

[24] **Malas, A., Pal, P., Das, C. K.** (2014). Effect of Expanded Graphite and Modified Graphite Flakes on the Physical and Thermo-Mechanical Properties of Styrene-Butadiene Rubber/Polybutadiene rubber blends. *Materials&Design, **55,*** 664-673.

[25] **Maiti, M., Srivastava, V. K., Shewale, S., Jasra, R. V., Chavda, A., Modi, S.** (2014). Process Parameter Optimization Through Design of Experiments in Synthesis of High *cis*-Polybutadiene Rubber. *Chemical Engineering Science, **107***, 256-265.

[26] **Wang, W., Zou, H-K., Chu, G-W., Weng Z., Chen J-F.** (2014). Bromination of Butyl Rubber in Rotating Packed Bed Reactor. *Chemical Engineering Journal*, ***240,*** 503-508.

[27] **Scagliusi S. R., Cardoso E. L. C., Lugao A. B.** (2012). Effect of Gamma Radiation on Chlorobutyl Rubber Vulcanized by Three Different Crosslinking Systems. *Radiation Physics and Chemistry*, ***81,*** 1370-1373.

[28] **Wegman, R. F., Twisk, J. V.** (2013). Rubbers in *Surface Preparation Techniques for Adhesive Bonding (2nd ed.*), 131-145, Elsevier Academic Press, Oxford, United Kingdom.

[29] **Cao Z-Qi., Wang D-G., Cong C-B., Wang Y-F., Zhou Q.** (2014). Dependence of Abrasion Behavior on Crosslinked Heterogeneity in Unfilled Nitrile Rubber. *Tribology International*, ***69,*** 141-149.

[30] **Dolbey, R**. (1997). Elastomer Types in *Polymeric Seals and Sealing Technology*, 17-20, Hickman J. A. (Ed.), Rapra Technology Ltd., Shropshire, United Kingdom.

[31] **Nabil, H., Ismail, H.** (2014). Blending of Natural Rubber/Recycled Ethylene-Propylene-Diene Rubber: Promoting the Interfacial Adhesion Between Phases by Natural Rubber Latex. *International Journal of Polymer Analysis and Characterization*, ***19,*** 159-174.

[32] **Perejón, A., Jiménez, P. E., González, E., Maqueda, L. A., Criado, J. M.** (2013). Pyrolysis Kinetics of Ethylene-Propylene (EPM) and Ethylene-Propylene-Diene (EPDM*). Polymer Degradation and Stability*, ***98,*** No:9, 1571-1577.

[33] **Keller R. W.** (1989). Oxidation and Ozonation of Rubber in *Handbook of Polymer Science and Technology* (*Vol. 2),* 143-165, Cheremisinoff, N. P. (Ed.), CRC Press.

[34] **Ning, N., Ma Q., Zhang Y., Zhang L., Wu H., Tian M.** (2014). Enhanced Thermo-Oxidative Aging Resistance of EPDM at High Temperature by Using Synergistic Antioxidants. *Polymer Degradation and Stability*, ***102,*** 1-8.

[35] **Cheremisinoff, N. P.** (1990). Principles and Methodology of Product Testing in *Product Design and Testing of Polymeric Materials*, 1-79, CRC Press, New York, The United States of America.

[36] **Endstra, W. C., Wreesmann C. T. J.** (1993). Peroxide Crosslinking of EPDM Rubbers in *Elastomer Technology Handbook*, 495-519, Cheremisinoff, N. P. (Ed.), CRC Press, Florida, The United States of America.

[37] **Karpeles, R., Grossi, A.** (2001). EPDM Rubber Technologhy in *Handbook of Elastomers (2nd ed.)*, 845-877, Bhowmick A. K., Stephens H. (Eds.), Marcel Dekker Inc., New York, The United States of America.

[38] **Ismail, H., Mathialagan, M.** (2012). Compatibilization of Bentonite Filled Ethylene-Propylene-Diene Monomer Composites: Effect of Maleic Anhydride Grafted EPDM. *Journal of Applied Polymer Science*, ***127,*** 1164-1171

[39] **Url-4** <*http://www.zorge.com/assets/Documents/Rubber-technology.pdf*>, date retrieved 17.03.2014.

[40] **Barlow, F. W.,** (1993). Reinforcers: Carbon Blacks in *Rubber Compounding: Principles: Materials, and Techniques (2nd Ed.)* , CRC Press, New York, The United States of America.

[41] **Xu, C., Wang, Y., Chen Y.** (2014). Highly toughened poly(vinylidene fluoride)/nitrile butadiene rubber blends prepared via peroxide-induced dynamic vulcanization. *Polymer Testing,* **33,** 179-186.

[42] **Blackley, D. C.** (1997). Rubber Vulcanizing Agents in *Polymer Latices (Vol.3) (2nd Ed.),* pp:35, T. J. International Ltd., London, United Kingdom.

[43] **Whelan T.** (1994). *Polymer Technology Dictionary (1st Ed.),* St. Edmundsbury Press, London, United Kingdom.

[44] **Url-5** <*http://www.ndsseals.com/rubber-ingredients.html*>, date retrieved 17.03.2014.

[45] **Melotto, M. A.** (1997). Mixing Machinery for Rubber in *The Mixing of Rubber (1st Ed.),* 1-20, Grossman, R.F. (Ed.), Florencetype Ltd., London, United Kingdom.

[46] **Gupta, B. R.** (1998). Mixing in *Rubber Processing On A Two-Roll Mill,* 15-56, Allied Publishers, New Delhi, India.

[47] **Cheremisinoff, N. P.** (1987). Banbury Mixers in *Polymer Mixing and Extrusion Technology,* CRC press, New York, The United States of America.

[48] **Kim, K-J., White, J. L**. (2010). Dispersion of Agglomerated Nanoparticles in Rubebr Processing in *Polymer Nanocomposites Handbook,* 123-147, Gupta, R. K., Kennel, E., Kim, K-J. (Eds.), CRC Press, The United States of America.

[49] **Twardowski T. E.** (2007). Nanocomposites Past and Future in *Introduction to Nanocomposite Materials: Properties, Processing, Characterization*, 1-8, DEStech Publications, Pennsylvania, The United States of America.

[50] **Koo, J. H.** (2006). An Overview of Nanoparticles in *Polymer Nanocomposites: Processing, Characterication and Applications*, 9-48, Manasreh, O. (Ed.), The McGraw-Hill Companies, Inc., The United States of America.

[51] **Rybiński, P., Janowska, G., Jóźwiak, M., Pająk A.** (2012). Thermal Stability and Flammability of Butadiene-Styrene Rubber Nanocomposites. *Journal of Thermal Analysis and Calorimetry, **109,*** No:2, 561-571.

[52] **Ismail, H., Pasbakhsh, P., Fauzi, M. N. A., Bakar, A. Abu** (2008). Morphological, Thermal and Tensile Properties of Halloysite Nanotubes Filled Ethylene Propylene Diene Monomer (EPDM) Nanocomposites. *Polymer Testing, **27,*** No:7, 841-850.

[53] **Ismail, H., Pasbakhsh, P., Fauzi, M. N. A., Bakar, A. Abu** (2009). The Effect of Halloysite Nanotubes as a Novel Nanofiller on Curing Behaviour, Mechanical and Microstructural Properties of Ethylene Propylene

Diene Monomer (EPDM) Nanocomposites. *Polymer-Plastics Technology and Engineering,* ***48,*** No:3, 313-323.

[54] **Ismail, H., Shaari, S. M.** (2010). Curing Characteristics, Tensile Properties and Morphology of Palm Ash/Halloysite Nanotubes/Ethylene-Propylene-Diene Monomer (EPDM) Hybrid Composites. *Polymer Testing,* ***29,*** No:7, 872-878.

[55] **Pasbakhsh, P., Ismail, H., Fauzi M. N. A., Azhar A. B.** (2009). The Partial Replacement of Silica or Calcium Carbonate by Halloysite Nanotubes as Fillers in Ethylene Propylene Diene Monomer Composites. *Journal of Applied Polymer Science,* ***113,*** No:6, 3910-3919.

[56] **Pasbakhsh, P., Ismail, H., Fauzi M. N. A., Azhar A. B.** (2009). Influence of Maleic Anhydride Grafted Ethylene Propylene Diene Monomer (MAH-g-EPDM) on the Properties of EPDM Nanocomposites Reinforced by Halloysite Nanotubes. *Polymer Testing,* ***2,*** No:5, 548-559

[57] **Pasbakhsh, P., Ismail, H., Fauzi M. N. A., Azhar A. B.** (2010). EPDM/Modified Halloysite Nanocomposites. *Applied Clay Science,* ***48,*** No:3, 405-413

[58] **Pasbakhsh, P., Ismail, H., Nor, A. F. M., Bakar, A. A.** (2012). Electron Beam Irradiation of Sulphur Vulcanised Ethylene Propylene Diene Monomer (EPDM) Nanocomposites Reinforced by Halloysite Nanotubes. *Macromolecular Engineering,* ***41,*** 430-440.

[59] **Guo, B. C., Chen, F., Lei Y. D., Liu X. L., Wan J. J., Jia D. M.** (2009). Styrene-Butadiene Rubber/Halloysite Nanotubes Composites Modified by Sorbic Acid. *Applied Surface Science,* ***255,*** 7329-7336.

[60] **Raman, V. S., Rooj, S., Das, A., Stöckelhuber, K. W., Simon, F., Nando, G. B., Heinrich, G.** (2013). Reinforcement of Solution Styrene Butadiene Rubber by Silane Functionalized Halloysite Nanotubes. *Journal of Macromolecular Science, Part A: Pure and Applied Chemistry,* ***50,*** 1091-1106.

[61] **Rooj, S., Das, A., Thakur, V., Mahaling, R.N., Bhowmick, A. K., Heinrich, G.** (2010). Preparation and Properties of Natural Nanocomposites Based on Natural Rubber and Naturally Occurring Halloysite Nanotubes. *Materials&Design,* ***31,*** No:4, 2151-2156

[62**] Ismail, H., Salleh, S. Z., Ahmad, Z.** (2013). Properties of Halloysite Nanotubes (HNT) Filled SMR L and ENR 50 Nanocomposites. *International Journal of Polymeric Materials and Polymeric Biomaterials,* **62,** No:6, 314-322.

[63] **Ismail, H., Salleh, S. Z., Ahmad, Z.** (2013). Properties of Halloysite Nanotubes Filled Natural Rubber Prepared Using Different Mixing Methods. *Materials and Design,* ***50,*** 790-797.

[64] **Ye, Y., Chen H., Wu J., Chan C. M.** (2011). Evaluation on the Thermal and Mechanical Properties of HNT-Toughened Epoxy/Carbon Fibre Composites. *Composites Part B: Engineering*, ***42,*** No:8, 2145-2150.

[65] **Soheilmoghaddam, M., Wahit M. U., Mahmoudian S., Hanid N. A.** (2013). Regenerated Cellulose/Halloysite Nanotube Nanocomposite Films Prepared with an Ionic Liquid. *Materials Chemistry and Physics*, ***141,*** No:2-3, 936-943.

[66] **Url-6 <***https://www.tut.fi/ms/muo/vert/9_test_methods/rubber_compounds_viscosity_and _scorch.htm***>**, date retrieved 28.03.2014.

[67] **Url-7** < *https://www.tut.fi/ms/muo/tyreschool/moduulit/moduuli_6/hypertext/3/3_4.html*>, date retrieved 28.03.2014.

[68] **Url-8** <*http://www.hawthornerubber.com/compression.html*>, date retrieved 28.03.2014.

[68] **Bhuvaneswari, C. M., Sureshkumar, M. S., Kakade, S. D., Gupta, M.** (2006). Ethylene-Propylene Diene Rubber as a Futuristic Elastomer for Insulations of Solid Rocket Motors. *Defence Science Journal*, ***56,*** No:3, 309-320.

[69] **Url-9** <*http://www1.odn.ne.jp/aal63880/CUTTER01-E.htm*>, date retrieved 28.03.2014.

[70] **Zhao, J., Ghebremeskel, G., Peasely, J.** (2001). Properties of EPDM/SBR Blends Cured with Peroxide and Sulfur Coagent. *Kautschuk Gummi Kunststoffe*, ***54,*** No:5, 223-228.

[71] **Yang, B.X., Shi, J.H., Pramoda, K.P., Hong Goh S.** (2007). Enhancement of Stiffness, Strength, Ductility and Toughness of Poly(ethylene oxide) Using Phenoxy-Grafted Multiwalled Carbon Nanotubes. *Nanotechnology*, ***18,*** 125606.

[72] **Stelescu, M-D., Manaila, E., Craciun, G., Dumitrascu M.** (2014). New Green Polymeric Composites Based on Hemp and Natural Rubber Processed by Electron Beam Irradiation. *Hindawi Publishing Corporation The Scientific World Journal*, ***2014,*** Article ID 684047, 1-13.

CURRICULUM VITAE

Name Surname : Yağmur POLAT

Place and Date of Birth : İstanbul - 20.04.1989

E-Mail : yagmurpolat1@gmail.com

EDUCATION:

B.Sc.: Hacettepe University / Department of Chemistry

M.Sc.: Istanbul Technical University / Polymer Science and Technology

Kaunas University of Technology / Faculty of Design and Technologies (Erasmus exchange student in the 4th semester of master)

PRESENTATIONS:

- **Polat, Y.,** Uyanık, N., 2013: Influence of Halloysite Nanotubes Contents on the Mechanical and Thermal Properties of EPDM Nanocomposites. *44th World Chemistry Congress,* August 11-16, 2013 Istanbul, Turkey.
- **Polat, Y.,** Uyanık, N., 2013: Influence of Halloysite Nanotubes Contents on the Mechanical and Thermal Properties of EPDM Nanocomposites. *1st International Symposium on Plastic and Rubber Technologies and Product Exhibition,* May 29-31, 2013 Ankara, Turkey.